

AD-A248 552



2

**NAVAL POSTGRADUATE SCHOOL**  
**Monterey, California**



**DTIC**  
**ELECTE**  
**APR 17 1992**  
**S D**

**THESIS**

Detection of Binary Phase Shift Keyed Signals in  
Extremely High Noise Levels

by

John B. Scout

March 1992

Thesis Advisor

Charles W. Therrien

Approved for public release; distribution is unlimited.

82 4 16 049

92-09841

Unclassified

Security Classification of this page

# REPORT DOCUMENTATION PAGE

1a Report Security Classification <b>Unclassified</b>		1b Restrictive Markings	
2a Security Classification Authority		3 Distribution Availability of Report <b>Approved for public release; distribution is unlimited.</b>	
2b Declassification/Downgrading Schedule		5 Monitoring Organization Report Number(s)	
4 Performing Organization Report Number(s)		7a Name of Monitoring Organization <b>Naval Postgraduate School</b>	
6a Name of Performing Organization <b>Naval Postgraduate School</b>	6b Office Symbol (If Applicable) <b>EC</b>	7b Address (city, state, and ZIP code) <b>Monterey, CA 93943-5000</b>	
6c Address (city, state, and ZIP code) <b>Monterey, CA 93943-5000</b>		9 Procurement Instrument Identification Number	
8a Name of Funding/Sponsoring Organization	8b Office Symbol (If Applicable)	10 Source of Funding Numbers	
8c Address (city, state, and ZIP code)		Program Element Number	Project No
		Task No	Work Unit Accession No
11 Title (Include Security Classification) <b>Detection of Binary Phase Shift Keyed Signals in Extremely High Noise Levels</b>			
12 Personal Author(s) <b>Scout, John B</b>			
13a Type of Report <b>Master's Thesis</b>	13b Time Covered From To	14 Date of Report (year, month, day) <b>1992 March</b>	15 Page Count <b>47</b>
16 Supplementary Notation <b>The views expressed in this thesis are those of the author and do not reflect the official policy or position of the Department of Defense or the U.S. Government.</b>			
17 Cosati Codes		18 Subject Terms (continue on reverse if necessary and identify by block number)	
Field	Group	Subgroup	
		<b>ESPRIT</b>	
19 Abstract (continue on reverse if necessary and identify by block number)			
<p>This thesis describes the design of a fully digital Binary Phase Shift Keyed receiver considered for use in a telemetry system in the range testing of torpedos. The method employed uses a subspace technique called Estimation of Signal Parameters via Rotational Invariant Techniques (<b>ESPRIT</b>) to detect the carrier frequency. This method can be used at lower than normal signal-to-noise ratio's. All results were achieved by the use of computer simulations.</p>			
20 Distribution/Availability of Abstract <input checked="" type="checkbox"/> unclassified/unlimited <input type="checkbox"/> same as report <input type="checkbox"/> DTIC users		21 Abstract Security Classification <b>Unclassified</b>	
22a Name of Responsible Individual <b>Charles W. Therrien</b>		22b Telephone (Include Area code) <b>(408) 646-3347</b>	22c Office Symbol <b>EC/Ti</b>

DD FORM 1473, 84 MAR

83 APR edition may be used until exhausted

All other editions are obsolete

security classification of this page

**Unclassified**

Approved for public release; distribution is unlimited.

Detection of Binary Phase Shift Keyed Signals in  
Extremely High Noise Levels

by

John B. Scout  
Lieutenant Commander, United States Navy  
B.S., United States Naval Academy, 1976

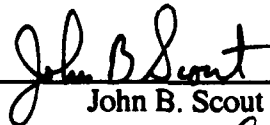
Submitted in partial fulfillment of the  
requirements for the degree of

MASTER OF SCIENCE IN ELECTRICAL ENGINEERING

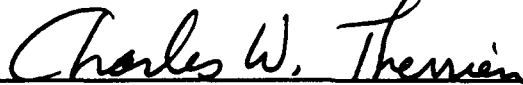
from the

NAVAL POSTGRADUATE SCHOOL  
March 1992

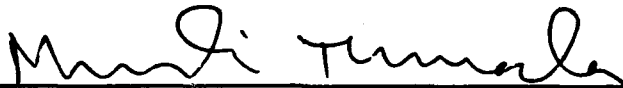
Author:

  
John B. Scout


Approved by:



Charles W. Therrien, Thesis Advisor



Murali Tummala, Second Reader



Michael A. Morgan, Chairman  
Department of Electrical and Computer Engineering

## ABSTRACT

This thesis describes the design of a fully digital Binary Phase Shift Keyed receiver considered for use in a telemetry system in the range testing of torpedos. The method employed uses a subspace technique called Estimation of Signal Parameters via Rotational Invariant Techniques (*ESPRIT*) to detect the carrier frequency. This method can be used at lower than normal signal-to-noise ratio's. All results were achieved by the use of computer simulations.

Accession For	
NTIS CRA&I	<input checked="" type="checkbox"/>
DTIC TAB	<input type="checkbox"/>
Unannounced	<input type="checkbox"/>
Justification .....	
By .....	
Distribution /	
Availability Codes	
Dist	Avail and/or Special
A-1	



## TABLE OF CONTENTS

I.	INTRODUCTION .....	1
A.	GENERAL .....	1
B.	OBJECTIVE.....	2
C.	ORGANIZATION .....	2
II.	BACKGROUND .....	3
A.	NATURE OF THE PROBLEM.....	3
B.	BPSK RECEIVERS.....	6
C.	ESPRIT.....	8
III.	EXPERIMENTAL PROCEDURE.....	12
A.	ASSUMPTIONS.....	12
B.	DESCRIPTION OF THE MODELING METHOD.....	14
C.	DESCRIPTION OF BPSK DEMODULATION TECHNIQUE .....	15
D.	DETERMINATION OF PERFORMANCE.....	21
IV.	SIMULATION RESULTS .....	23
A.	ACCURACY OF ESPRIT .....	23
B.	PROBABILITY OF BIT ERROR.....	34
V.	CONCLUSIONS AND RECOMMENDATIONS .....	40
A.	CONCLUSIONS.....	40
B.	RECOMMENDATIONS .....	40
	LIST OF REFERENCES .....	41
	INITIAL DISTRIBUTION LIST.....	42

# **I. INTRODUCTION**

## **A. GENERAL**

Over the past twenty years, there has been an almost continuous shift in emphasis from analog to digital electronics. This shift is most readily seen in what have become common household appliances such as VCR's, stereos and computers. One has but to read the daily newspapers to get a true feel for this new and digitized world we live in. Every new method or technique that is developed to manipulate and process digital information is rapidly investigated and then incorporated into the latest state of the art equipment. Indeed, that seems to be the selling point of over 90% of the electronics on the market today.

This thesis deals with the use of one of the newer subspace techniques, *ESPRIT* (Estimation of Signal Parameters via Rotational Invariant Techniques), in the detection of sinusoidal signals in a high noise level environment. The technique was originally designed for the determination of direction of arrival as well as other signal parameters and assumed an array of sensors [Ref. 1:p. 1]. However, for the purposes of this thesis, a single sensor is used and the parameter of interest is the frequency of the received signal.

The specific application investigated by this thesis is the demodulation of Binary Phase Shift Keyed (BPSK) acoustic signals in the presence of high background noise. The noise is generated by an acoustic countermeasure and hinders the detection and demodulation of the BPSK signal. The BPSK signal itself is transmitted from a torpedo and carries telemetry data which is used by the control center of the test range. A doppler shift in the transmitted signal occurs as a result of the torpedo velocity and ocean currents. Therefore, detection of the frequency of the received signal is critical to the demodulation process.

## **B. OBJECTIVE**

The objective of this thesis was to study the possibility of using linear algebraic subspace techniques for the demodulation of a BPSK signal in the presence of high noise levels. This required a determination of the accuracy of the detected frequency and an estimation of the probability of bit error ( $P_e$ ) of the demodulated BPSK signal. Since all of this was investigated in the context of the torpedo tracking problem, it was also necessary to accurately simulate existing hardware components and the broadband noise generated by the acoustic countermeasure.

## **C. ORGANIZATION**

The remainder of this thesis is organized as follows: Chapter II discusses the background needed to fully understand the nature of the problem presented in this thesis. A basic description of the problem area is first presented. This is followed by a review of BPSK receivers and a description of the *ESPRIT* algorithm. Chapter III describes the experimental procedure used in this thesis, the assumptions made, and their justification. The modeling method used for the computer simulations is also described. This includes the specific BPSK demodulation technique that was implemented and the method used to determine the performance of the BPSK receiver. Chapter IV provides the main results of the research. Included in the results are the accuracy of the *ESPRIT* algorithm in this application and the estimated probability of bit error. Chapter V presents conclusions and recommendations.

## **II. BACKGROUND**

### **A. NATURE OF THE PROBLEM**

The Naval Undersea Warfare Center (NUWC) at Keyport, Washington conducts various types of underwater tracking exercises as part of its research and development activities. Each vehicle being tracked on one of the NUWC acoustic ranges has a transmitter installed. The function of this transmitter is twofold. The first is to allow accurate real-time tracking of the three-dimensional position of the vehicle. The second function of the transmitter is to send telemetry data from the vehicle to the control center. This telemetry data is transmitted at a carrier frequency of 75 kilohertz (kHz) using BPSK modulation. Specifically, each telemetry transmission consists of 47 bits of data. Each bit is seven cycles of the carrier in length, or 93.33  $\mu$ sec, for a total data stream length of 43.387 msec. The first five bits are always a "1" to help in synchronization. Figure 2-1 is an example of what three bits of the data stream, representing 1 1 0, might look like.

The NUWC range is instrumented with sensor arrays that are approximately 2000 yards apart. Each array consists of four hydrophones that are used to determine direction of arrival of the BPSK signal. Only one array at a time is normally used for tracking. Figure 2-2 shows one of the NUWC ranges for which this problem was studied.

As part of ongoing research and development projects, NUWC has been conducting experiments on torpedoes in the presence of acoustic countermeasures. This has increased the difficulty of both the tracking of the torpedo and the demodulation of the BPSK signal due exclusively to the decrease in the signal-to-noise ratio (SNR). The research problem addressed in this thesis is how to accurately detect and demodulate this BPSK signal while in the presence of the high noise level associated with the acoustic countermeasures.

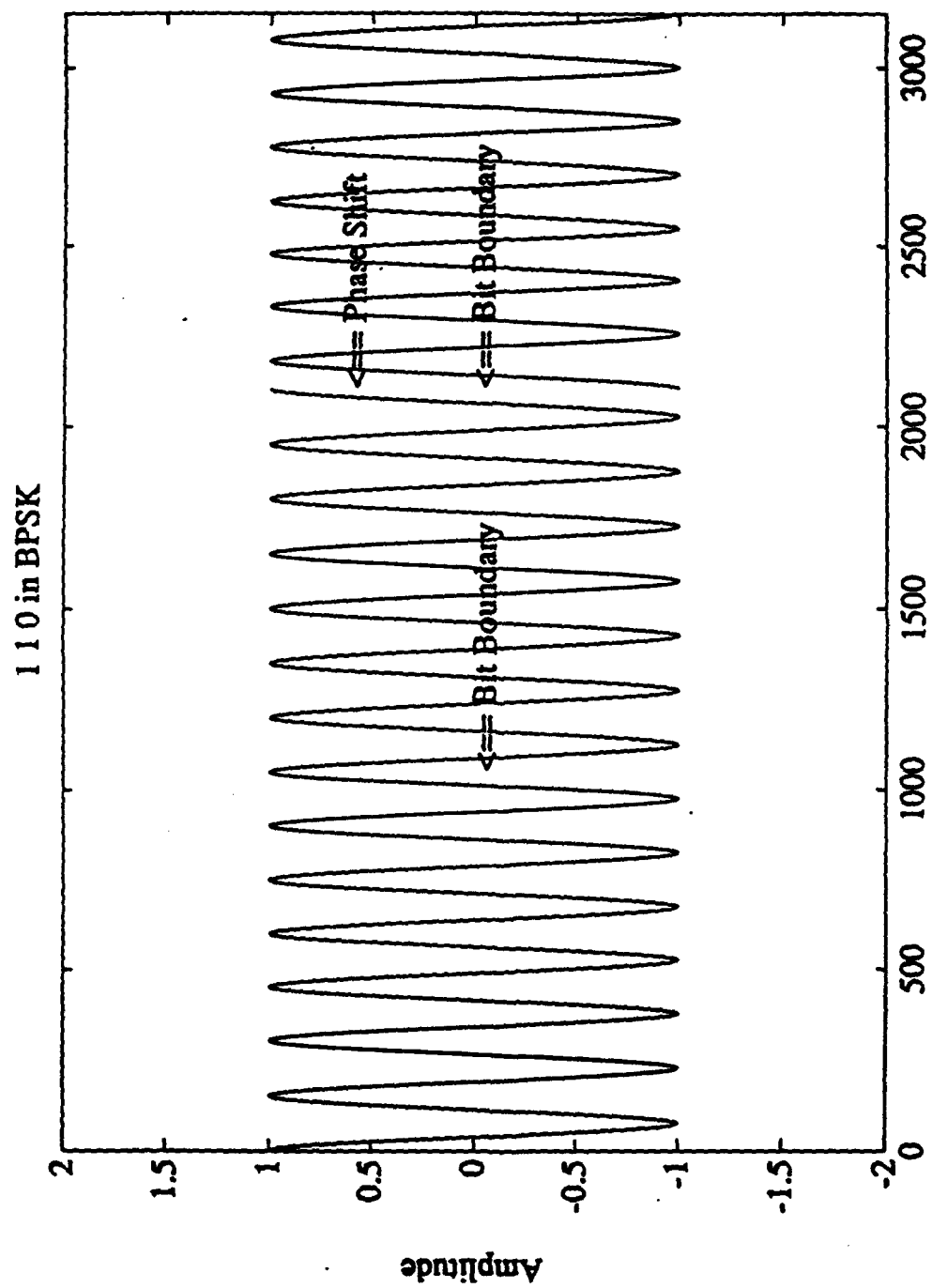


Figure 2-1. BPSK Signal for a Binary Code of 1 1 0

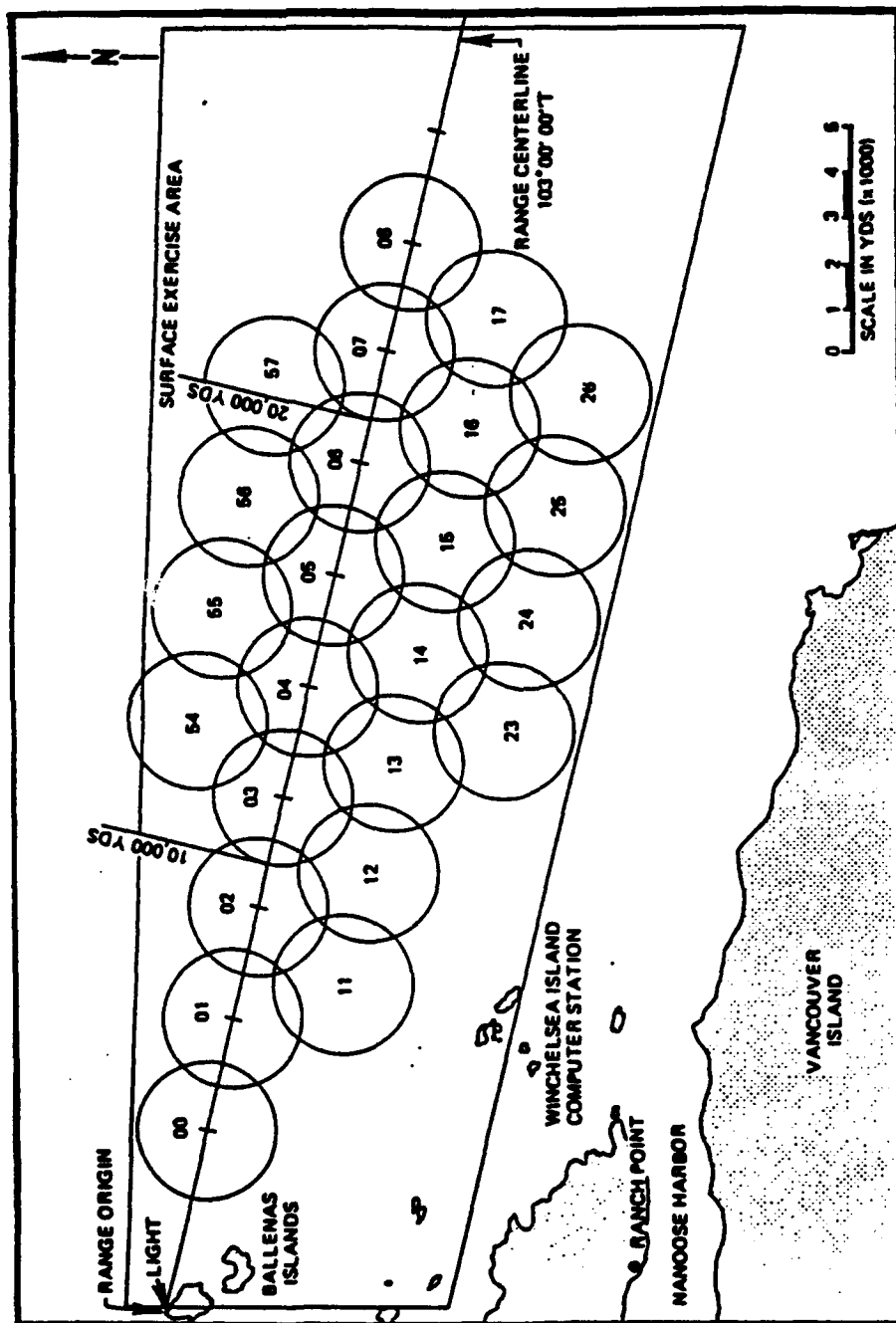


Figure 2-2. Configuration of a NUWC Test Range  
(Drawing courtesy of Code 70E NUWC)

## B. BPSK RECEIVERS

Since the data transmission involves BPSK modulation, it is appropriate here to review the basic concepts of BPSK modulation and demodulation schemes. For BPSK modulation, the binary coded data sequence is represented by one of two possible outputs:  $s_1(t) = A\cos(2\pi f_c t)$  and  $s_2(t) = A\cos(2\pi f_c t + \pi) = -A\cos(2\pi f_c t)$ . The signal  $s_1(t)$  is transmitted when a "1" is to be sent and  $s_2(t)$  is transmitted when a "0" is to be sent. The bit stream of the message being sent is made up of a constant number of cycles of  $s_1(t)$  and  $s_2(t)$ . This signal is corrupted by noise in the transmission channel. The BPSK receiver must remove as much noise as possible and then demodulate the remaining signal to recover the bit stream of "1"s and "0"s.

Figure 2-3 [Ref. 2:p. 245] shows a typical block diagram of a BPSK demodulator. This type of demodulation is referred to as coherent detection because it requires the recovery of both the frequency and the phase of the carrier. The received signal has the form  $A\cos(2\pi f_c t + B(t)) + \eta(t)$  where  $f_c$  is the carrier frequency,  $B(t)$  is the carrier phase (either 0 or  $\pi$ ) and  $\eta(t)$  is the additive noise. The received signal is sent through a bandpass filter centered at the nominal carrier frequency. This removes as much noise as possible. The filtered signal is then multiplied by  $\cos(2\pi f_c t + B(t))$ . This results in a signal of the form  $A/2 + (A/2)\cos(4\pi f_c t + 2B(t)) + \eta(t)\cos(2\pi f_c t + B(t))$ , which is then integrated and sampled. (This has the same effect as sending it through a low pass filter and then sampling it.) The output of the sampler (disregarding the noise) is the direct current (DC) value  $\pm A/2$  where a positive value means a "1" was sent and a negative value means a "0" was sent. Any error in the synchronization of the carrier phase or in

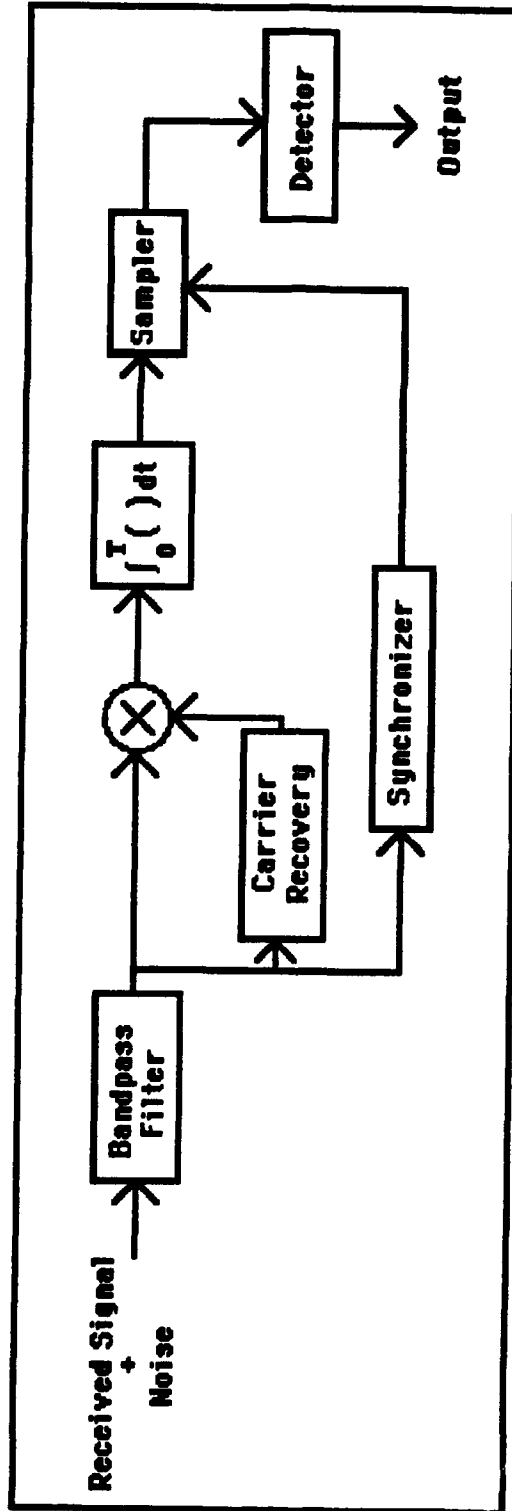


Figure 2-3. Block Diagram of a Typical BPSK Receiver

the detection of the carrier frequency may cause errors in the demodulated output. The magnitude of phase error, which can be tolerated, decreases as the SNR of the received signal decreases [Ref. 2:p. 345]. As will be shown in detail later, the frequency error that can be tolerated is very small.

When a situation occurs such that the noise power is much greater than the signal power (i.e. negative SNR), it may not be possible to recover the signal using the standard type of receiver. This thesis investigates one possible alternative to the demodulation of BPSK signals in the presence of high noise levels.

### C. *ESPRIT*

The *ESPRIT* algorithm was developed by R. H. Roy et al in 1987 at Stanford University [Ref. 1:p. vii-viii]. The basic idea behind *ESPRIT* is the use of the rotational invariance associated with signal subspaces to detect the parameters of a signal in noise [Ref. 1:p. v]. Three forms of the *ESPRIT* algorithm have been reported in the literature. The first, which will be referred to as "basic" *ESPRIT*, was initially studied in this work because it is the simplest to apply and analyze [Ref. 3:p. 638-649]. Two other related forms known as least squares *ESPRIT* and total least squares (TLS) *ESPRIT* have also been described [Ref. 3:p. 638-649]. Each form is progressively more elegant in its formulation and has correspondingly better performance. Since our final results involve only TLS *ESPRIT*, it is the only form that will be discussed here. The TLS *ESPRIT* method will therefore be referred to simply as *ESPRIT*.

The idea of separating a signal into two subspaces to estimate complex exponentials was developed in the 1970's. The theory states that the vector space in which a signal consisting of complex exponentials plus noise resides is composed of two subspaces, a "signal" subspace and a "noise" subspace. The eigenvector decomposition (or generalized eigenvector decomposition) of the correlation matrix correspondingly yields

two sets of eigenvectors and eigenvalues. The eigenvectors corresponding to the smallest valued eigenvalues (which are all equal to the same constant value) represent the noise subspace while the remaining eigenvectors represent the signal subspace. Although none of the signal vectors lie in the noise subspace, a part of the noise vectors lie in the signal subspace. When the noise is white, the eigenvectors representing the signal subspace contain a complex exponential which can be used to estimate the signal frequency. When the noise is not white, the signal subspace eigenvectors can be transformed into basis vectors that contain the complex exponential. In the *ESPRIT* algorithm, two such subspaces are considered, one corresponding to a given set of  $N$  samples of the signal and the other corresponding to a set of  $N$  samples shifted by one. Corresponding eigenvectors of the two signal subspaces differ by a constant factor  $e^{j\omega_i}$  where  $\omega_i$  corresponds to the  $i^{\text{th}}$  signal subspace eigenvector. The goal of the *ESPRIT* algorithm is to extract the parameters  $\omega_i$  through linear algebraic operations. [Ref. 3:p. 638-649]

In the BPSK application, it is the frequency of the received signal that must be accurately determined in order to perform the demodulation. The *ESPRIT* algorithm is employed to estimate the frequency through the steps presented below.

A vector  $\mathbf{x}$  is defined which consists of  $N+1$  samples of data, that is,  $\mathbf{x} = [x(0) \ x(1) \ \dots \ x(N)]^T$ . This data is comprised of both signal and noise. From this vector of data samples, an estimated correlation matrix,  $\hat{\mathbf{R}}_x$ , is computed. Because of the small amount of data, either the covariance method or the modified covariance method should be used for the computation to avoid any unnecessary bias [Ref. 3:p. 648]. *ESPRIT* makes the assumption that the statistical characteristics of the noise are either known or can be estimated. From these statistics, the estimated (or actual, if known)

noise correlation matrix,  $\Sigma_n$ , is computed. Using these two correlation matrices, the generalized eigenvectors and eigenvalues of  $\hat{R}_x$  are computed from:

$$\hat{R}_x \mathbf{g}_k = \lambda_k \Sigma_n \mathbf{g}_k$$

where  $\mathbf{g}_k$  is the  $k^{\text{th}}$  eigenvector and  $\lambda_k$  is the corresponding eigenvalue. If the number of signals present is unknown, it can be estimated from the resulting matrix of eigenvalues (see [3]). A basis which spans the signal subspace,  $\mathbf{B}$ , is then generated from the noise correlation matrix and the eigenvectors  $\mathbf{g}$  and partitioned into two matrices,  $\mathbf{B}_1$  and  $\mathbf{B}_2$  (see summary below).  $\mathbf{B}_1$  represents a basis for the signal subspace corresponding to the unshifted data samples  $x(0) \dots x(N-1)$ , and  $\mathbf{B}_2$  represents a corresponding basis for the set of shifted signal samples  $x(1) \dots x(N)$ . The two bases are related as

$$\mathbf{B}_1 \Psi = \mathbf{B}_2 \quad (2-1)$$

where  $\Psi$  is a suitable transformation. The eigenvalues of  $\Psi$  are complex exponentials  $e^{j\omega_i}$ , which contain the desired frequencies.

Since equation (2-1) is not satisfied exactly for experimentally measured data, an *approximate* solution needs to be found. In TLS *ESPRIT*, the solution is obtained via the method of total least squares. A derivation and discussion of the TLS method can be found in Theorem 12.2.1 in Golub and Van Loan [Ref. 4]. The matrix  $\mathbf{V}$  of right singular vectors of a new matrix  $[\mathbf{B}_1 \mathbf{B}_2]$  is computed and partitioned into four square matrices such that:

$$\mathbf{V} = \begin{bmatrix} \mathbf{V}_{11} & \mathbf{V}_{12} \\ \mathbf{V}_{21} & \mathbf{V}_{22} \end{bmatrix}$$

where each of the partitions is a square with dimension equal to the number of signals  $M$ .

The eigenvalues of  $-\mathbf{V}_{12}\mathbf{V}_{22}^{-1}$  are then computed. These eigenvalues are complex, and the angles of the eigenvalues are the radian frequencies of the signals [Ref. 3:p. 638-649]. A summary of the algorithm is as follows:

- \* Define the vector of data samples  $\mathbf{x} = [x(0), x(1), \dots, x(N)]^T$  and compute the correlation matrix  $\hat{\mathbf{R}}_{\mathbf{x}}$ . This is the correlation matrix of the combined signal plus noise.
- \* Compute the generalized eigenvectors and eigenvalues of  $\hat{\mathbf{R}}_{\mathbf{x}}$  from  $\hat{\mathbf{R}}_{\mathbf{x}}\mathbf{e}_k = \lambda_k \Sigma_{\mathbf{x}} \mathbf{e}_k$ .
- \* If necessary, estimate the number of signals present from the eigenvalues. (If the number of signals is already known as in our application, this step can be skipped.) This is the number  $M$  and determines the number of columns of eigenvectors to use in forming matrix  $\mathbf{B}$  in the next step.
- \* Generate the basis which spans the signal subspace:  $\mathbf{B} = \Sigma_{\mathbf{x}} \mathbf{e} = \begin{bmatrix} \mathbf{B}_1 \\ \mathbf{x} \\ \mathbf{B}_2 \end{bmatrix} = \begin{bmatrix} \mathbf{x} \\ \mathbf{B}_2 \end{bmatrix}$  where  $\mathbf{x}$  denotes the first or last row of  $\mathbf{B}$  and is not used in defining  $\mathbf{B}_2$  and  $\mathbf{B}_1$  respectively. This eliminates the noise subspace from the computations.
- \* Compute matrix  $\mathbf{V}$  of right singular vectors by taking the SVD of the matrix  $[\mathbf{B}_1 \ \mathbf{B}_2]$ .
- \* Partition  $\mathbf{V}$  such that  $\mathbf{V} = \begin{bmatrix} \mathbf{V}_{11} & \mathbf{V}_{12} \\ \mathbf{V}_{21} & \mathbf{V}_{22} \end{bmatrix}$ .
- \* Compute the complex eigenvalues of  $-\mathbf{V}_{12}\mathbf{V}_{22}^{-1}$ . The last three steps combine to solve the total least squares problem.
- \* Find the signal frequencies  $\omega_k = \angle \lambda_k$  where  $k = 1, 2, \dots, M$  is the number of signals present. The angle of the complex eigenvalues provides an estimate for the radian frequency of the signals. The magnitude of the eigenvalues should be very close to one. [Ref. 3:p. 648]

In this thesis, the *ESPRIT* algorithm is used to detect the frequency of the received signal. This frequency is then used to demodulate the received signal, providing the decoding of the telemetry data.

### III. EXPERIMENTAL PROCEDURE

#### A. ASSUMPTIONS

This chapter deals specifically with the application of *ESPRIT* to the frequency estimation problem involved in the BPSK demodulation on the NUWC ranges. This first section discusses the assumptions made during the investigation and gives the justification for making those assumptions. Recall that, in the torpedo tracking problem, the signal is observed in the presence of interference from an acoustic countermeasure.

The first assumption in the analysis is that the acoustic countermeasure is additive white noise (AWN). This assumption is considered valid because the countermeasure produces high levels of noise over a very wide band. Over the relatively narrow bandwidth of the array hydrophone and preamplifier (65 - 85 kHz), the broadband noise produced by the countermeasure has an approximately flat power spectral density.

Another assumption made regarding the noise is that the correlation matrix of the colored noise at the output of the hydrophone and preamplifier can be estimated directly from the filter weights of the hydrophone and preamplifier. The combination of hydrophone and preamplifier is just a bandpass filter with filter weights  $h(n)$ . If the input is  $x(n)$  and the output is  $y(n)$ , then the correlation function of the output is  $R_y(m) = h(m) * h(-m) \cdot R_x(m)$ , where  $*$  represents convolution and for white noise,  $R_x(l) = \sigma^2 \delta(l)$  [Ref. 3]. This yields a correlation matrix which is just a Toeplitz matrix of the correlation function  $R_y(m)$ . For the case where the filtered and sampled signal is squared, the correlation vector used for the noise was computed from

$$R_{y2}(m) = h^2(n) * h^2(n-m) \cdot 3\sigma^4.$$

This can be derived as follows . The filter output is given by the convolution

$$y(n) = \sum_k h(n-k)w(k)$$

where  $w(k)$  is the noise sequence and  $h(n)$  is the filter impulse response. Then the squared output is

$$y^2(n) = \left\{ \sum_k h(n-k)w(k) \right\} \left\{ \sum_j h(n-j)w(j) \right\}. \quad (3-1)$$

The correlation function is defined by

$$R_y\chi(m) = E[y^2(n)y^2(n-m)].$$

Substituting into (3-1) and expanding we have

$$R_y\chi(m) = E\left[\left(\sum_k \sum_j h(n-k)h(n-j)w(k)w(j)\right)\left(\sum_p \sum_q h(n-m-p)h(n-m-q)w(p)w(q)\right)\right]$$

$$R_y\chi(m) = \sum_k \sum_j \sum_p \sum_q h(n-k)h(n-j)h(n-m-p)h(n-m-q) \cdot E[w(k)w(j)w(p)w(q)].$$

Now observe that  $E[w(k)w(j)w(p)w(q)]$  equals zero unless  $k = j = p = q$ . Therefore the last equation simplifies to

$$R_y\chi(m) = \sum_k h(n-k)h(n-k)h(n-m-k)h(n-m-k) \cdot E[w^4(k)]$$

$$R_y\chi(m) = \sum_k h^2(n-k)h^2(n-m-k) \cdot E[w^4(k)].$$

Since for Gaussian white noise  $E[w^4(k)] = 3\sigma^4$ , it follows that

$$R_y\chi(m) = h^2(n) * h^2(n-m) \cdot 3\sigma^4.$$

The next assumption is that multipath propagation of the signal bit stream does not cause any significant interference. This is valid since the geometry of the NUWC acoustic range is such that only the direct path signal arrives during the duration of the bit stream (43.387 msec). (This has been verified experimentally by NUWC.) Furthermore, any multipath noise signals from previous bit streams are uncorrelated with the noise in the current bit stream and simply adds to its variance.

The final assumption is that some method of synchronization with the first bit can be achieved. This is considered a valid assumption because of the plethora of correlators and synchronization methods currently in use.

## **B. DESCRIPTION OF THE MODELING METHOD**

All modeling was carried out using MATLAB™ software and MATLAB built in functions. The AWN was simulated by using a random number generator with a normal distribution. The mean of the normal distribution was zero and the variance ( $\sigma^2$ ) was determined from the desired SNR (in dB),  $\sigma^2 = 10^{-(\text{SNR}/10)}$ . This assumes that the amplitude of the carrier is unity.

The array hydrophone and preamplifier with its 20 kHz bandwidth was simulated by using a digital 12th order Butterworth bandpass filter. Figure 3-1 is a plot of the magnitude and phase characteristics of the array hydrophone and preamplifier. Figure 3-2 is a plot of the magnitude and phase characteristics of the 12th order Butterworth filter. As can be seen from the figures, the Butterworth filter is a reasonable approximation of the array hydrophone and preamplifier.

Using the filter weights from the Butterworth filter mentioned above, the noise correlation matrix  $\Sigma_{\eta}$  was generated as discussed in the assumptions. This was needed because of the coloring effect of passing the AWN through the bandpass filter.

The telemetry signal was generated as a sampled cosine wave with a constant sampling rate of 600 kHz. In order to simulate a continuous signal with correct doppler shift of the signal due to the torpedo velocity, the cosine wave was initially generated using a sampling rate ( $f_{s1}$ ) that was an integer multiple of both 600 kHz and the desired doppler shifted frequency. This sampling frequency was typically on the order of 12 MHz. The cosine wave was one bit long, and the entire bit stream was then generated by

multiplying that single prototype bit by a 1 or a -1 and then concatenating the bits together. To obtain the final waveform for the signal, every  $K^{\text{th}}$  data point was retained where  $K = f_{s1} / 600 \text{ kHz}$ . In the example above,  $K = 12 \text{ MHz} / 600 \text{ kHz} = 20$ .

### C. DESCRIPTION OF BPSK DEMODULATION TECHNIQUE

The first step in the demodulation process was to sample the received signal at a rate of 600 kHz. This sampled signal was then applied to the bandpass filter, and the *ESPRIT* algorithm was applied to the output. From the *ESPRIT* algorithm, the frequency of the received signal was estimated. Two methods were used to do this. The first method was to use the first five bits as inputs to the *ESPRIT* algorithm to determine the frequency. The second method was to square the incoming signal and use most of the 47 bits. The 47 bits were broken into groups of three, five, or seven, and each group was successively applied to the *ESPRIT* algorithm. The results of this were then averaged to reduce the variance of the results. This required a temporary storage of the original sampled signal. Since the form of the carrier is known to be a cosine wave, a second demodulation signal is generated as  $\cos(\hat{\omega}_0 n + \phi)$ . This demodulation signal is multiplied by the received signal on a bit by bit basis to minimize errors caused by inaccuracies in the frequency estimate. This generates a DC component and a double frequency component at  $2\omega_0$ . The discrete Fourier transform (DFT) of this signal is then taken, and the double frequency portion of the spectrum is zeroed out. This has the effect of lowpass filtering. The inverse DFT is then taken, and the average value of the signal over the bit lengths is computed. If the average value of the signal is positive, then that bit is evaluated as a "1"; if the average value is zero or negative, it is decoded as a "0". Figure 3-3 shows a block diagram of this demodulation technique.

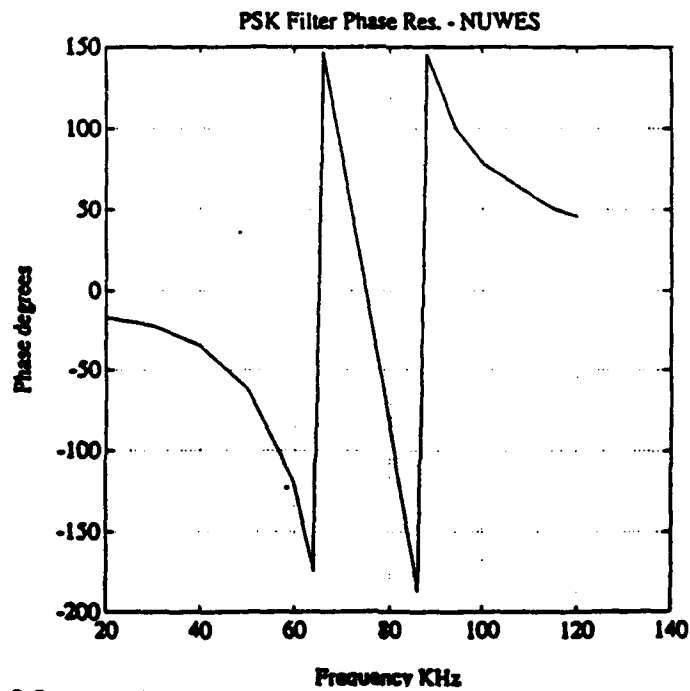
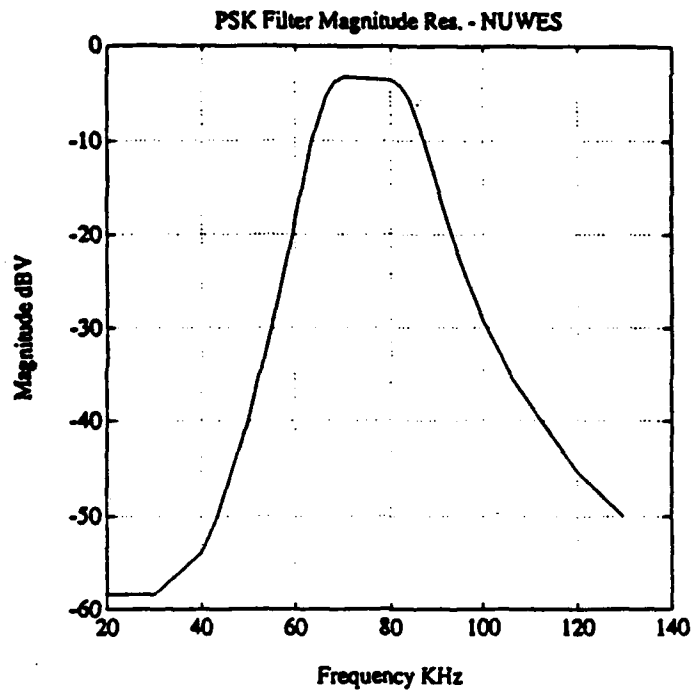


**Figure 3-1. Magnitude and Phase Response of NUWC Array Hydrohone and Preamplifier**

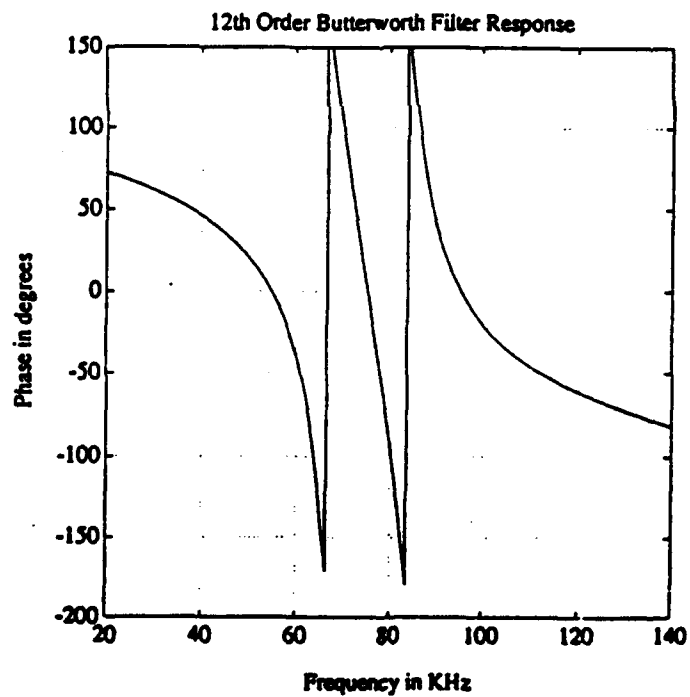
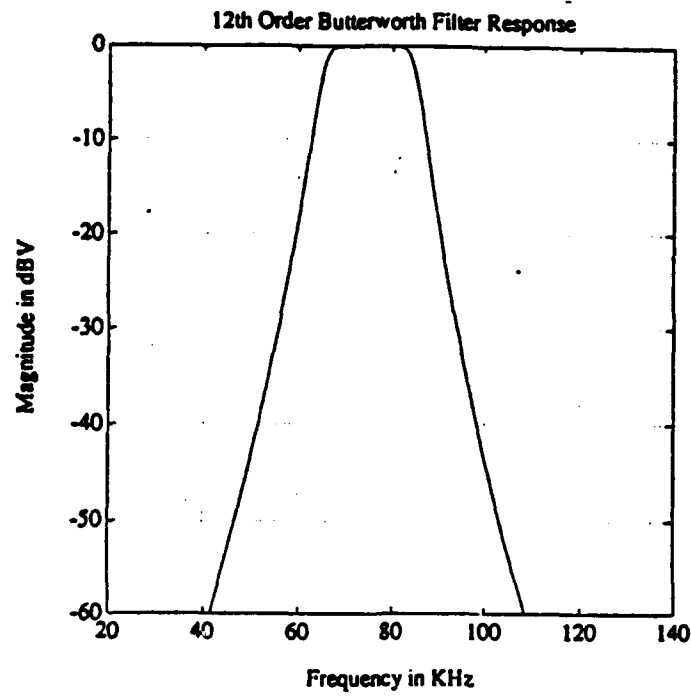


**Figure 3-2. Magnitude and Phase Response of a 12th Order Butterworth Filter**

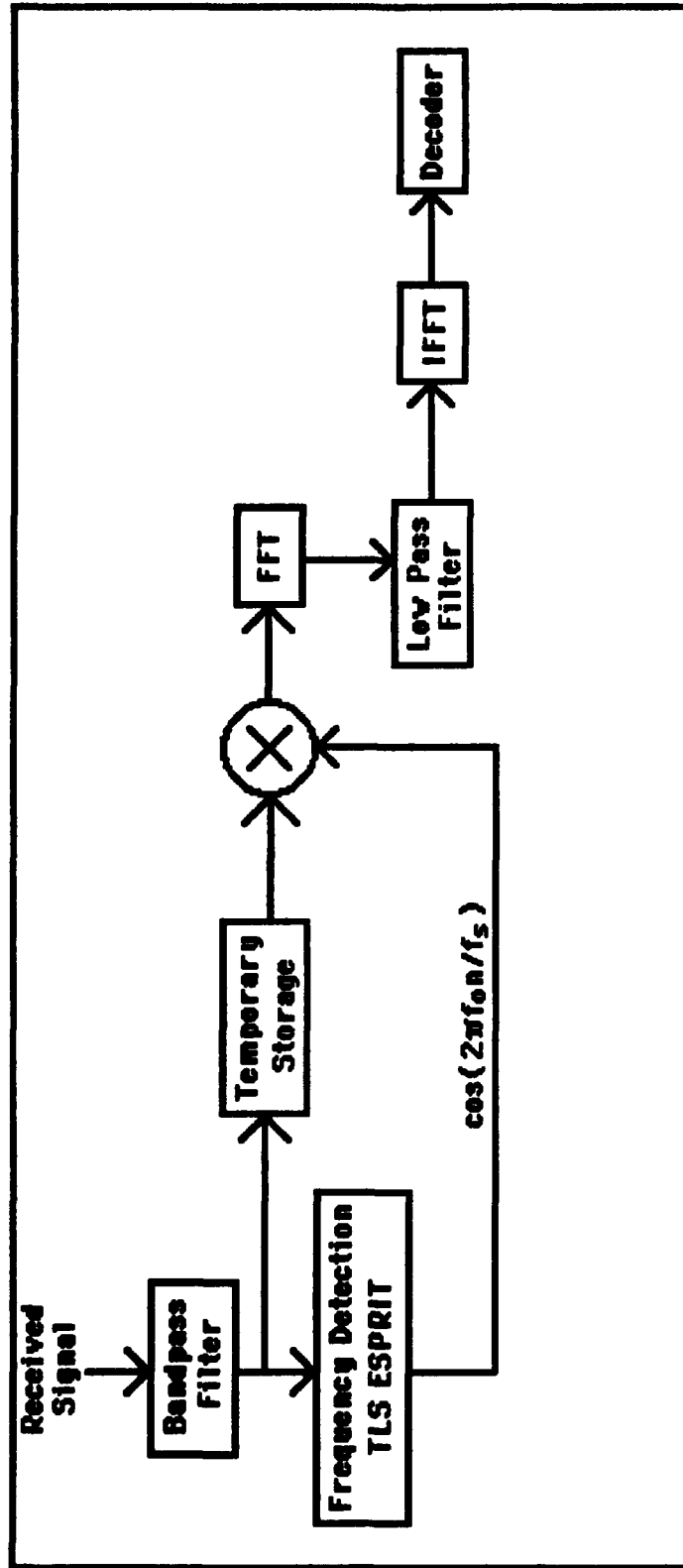


Figure 3-3. Block Diagram of BPSK Demodulation Method

The difficulty here is in determining the bit boundaries between which the average is taken. For a constant sampling rate of 600 kHz and a worst case received frequency of 80 kHz, the largest number of samples that can be averaged for one bit is  $600 \cdot 7/80 - 1 = 51$ . (The  $-1$  is to allow for the unknown phase.) For each bit, the problem is determining which particular sample of the received data is the first sample for that bit. In addition, if the first sample for a bit does not fall on the bit boundary, a phase offset must be determined to account for the time difference between the actual start of the bit and the first sample. This occurs because the sampling rate is not an integral multiple of the received frequency and the samples do not necessarily fall on the bit boundaries. To show how this was accomplished, a few definitions are in order. Figure 3-4 shows the relationships between the following terms.  $T_r$  is the period of one cycle of the received signal, i.e.,  $T_r = 2\pi/\omega_0$ . The variable  $\Delta t$  is the time from the last sample used of a bit to the end of that bit while  $\Delta t'$  is the time from the start of the next bit until the first sample. The quantity  $\phi$  is the phase offset at the start of a bit and  $T_s$  is the sampling period equal to  $1.67 \mu\text{sec}$ . Finally,  $n$  is the index of the first sample of the next bit while  $n'$  is the index of the last sample used of the previous bit. Each bit is computed on an iterative basis as follows:

- \*  $\Delta t(k+1) = 7T_r - \Delta t'(k) - 50T_s$
- \*  $\Delta t'(k+1) = T_s - \Delta t(k+1) + \lfloor (\Delta t(k+1) / T_s) \rfloor T_s$  where  $\lfloor \cdot \rfloor$  is just the number rounded down to the next lowest integer.
- \*  $\phi(k+1) = \Delta t'(k+1)2\pi / T_r$
- \*  $n = n' + \{\Delta t(k+1) + \Delta t'(k+1)\} / T_s$

This allows the sampled received signal to be broken down into individual bits for demodulation and recovery when the transmitted signal has been effected by doppler.

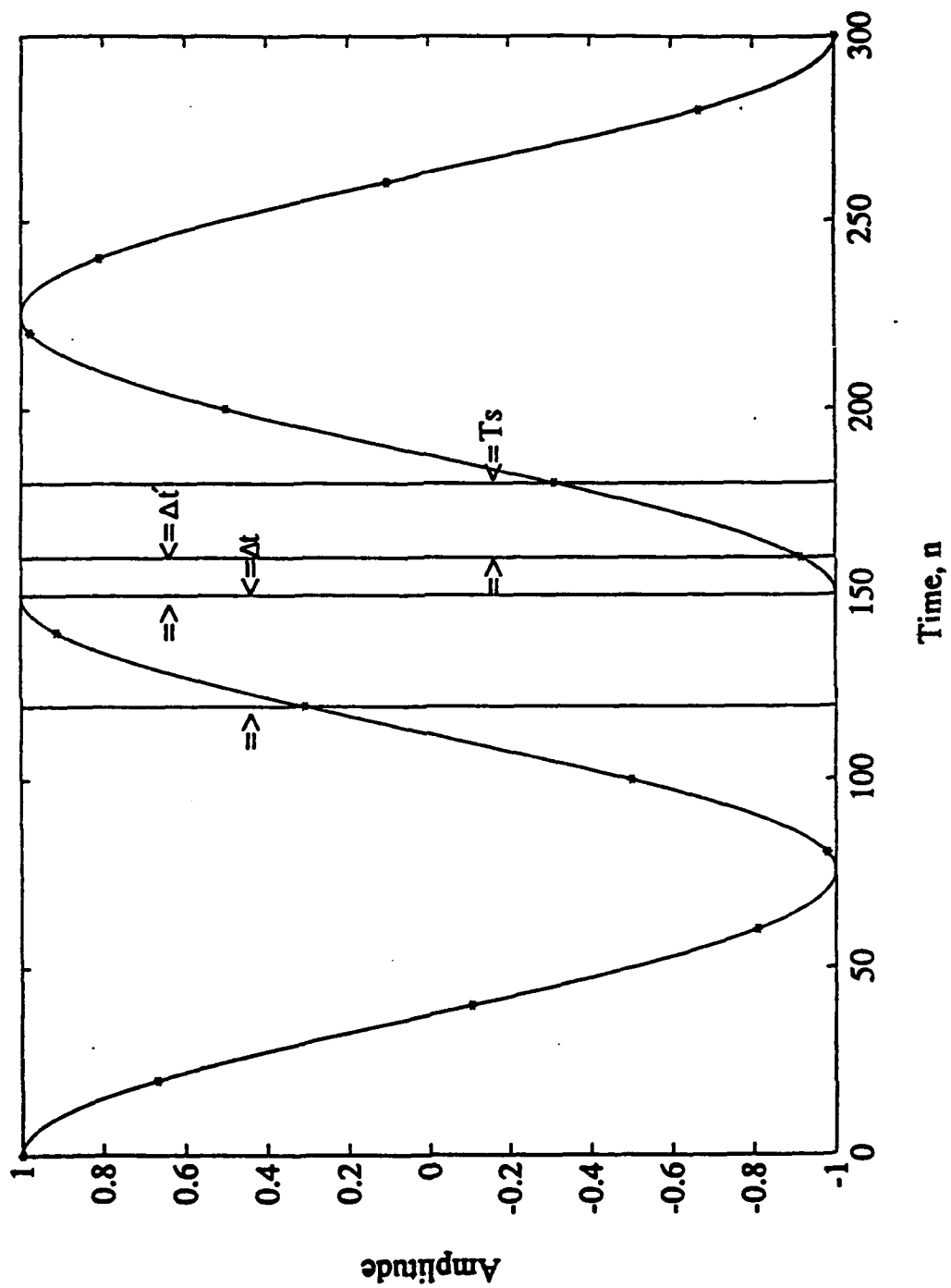


Figure 3-4. Determination of Bit Boundaries

When there is no doppler present and the sampling rate is an integral multiple of the transmitted frequency, the problem becomes much simpler. The bit boundaries are then known since each bit has exactly  $f_s/f_r$  samples. In this case, extremely high accuracy for the frequency estimate is *not required* because there is no computation of the bit boundary from the estimate. Since each bit boundary is known precisely, there is no accumulation of errors in computing bit boundaries, and consequently, no decoding errors due to this effect. The results are given in the next chapter.

#### **D. DETERMINATION OF PERFORMANCE**

In order to determine the adequacy of the *ESPRIT* algorithm as a BPSK demodulation technique, a method had to be derived for evaluating its performance. The first step in this process was to determine the accuracy needed to demodulate the BPSK signals. Using a large value for SNR (100 dB), a BPSK signal was demodulated for various assumed carrier frequencies. Figure 3-5 shows that in order to obtain no errors, the carrier frequency estimate must be accurate to within +40 Hz to -60 Hz. This is the case when doppler is present because of the accumulation of errors in computing the phase offset. When there is no doppler present and the sampling rate is very nearly an integer multiple of the carrier frequency, a much larger error in estimating the carrier frequency can be tolerated as discussed above. This is true because the bit boundaries are known, and there is no phase offset error accumulation for the individual bits.

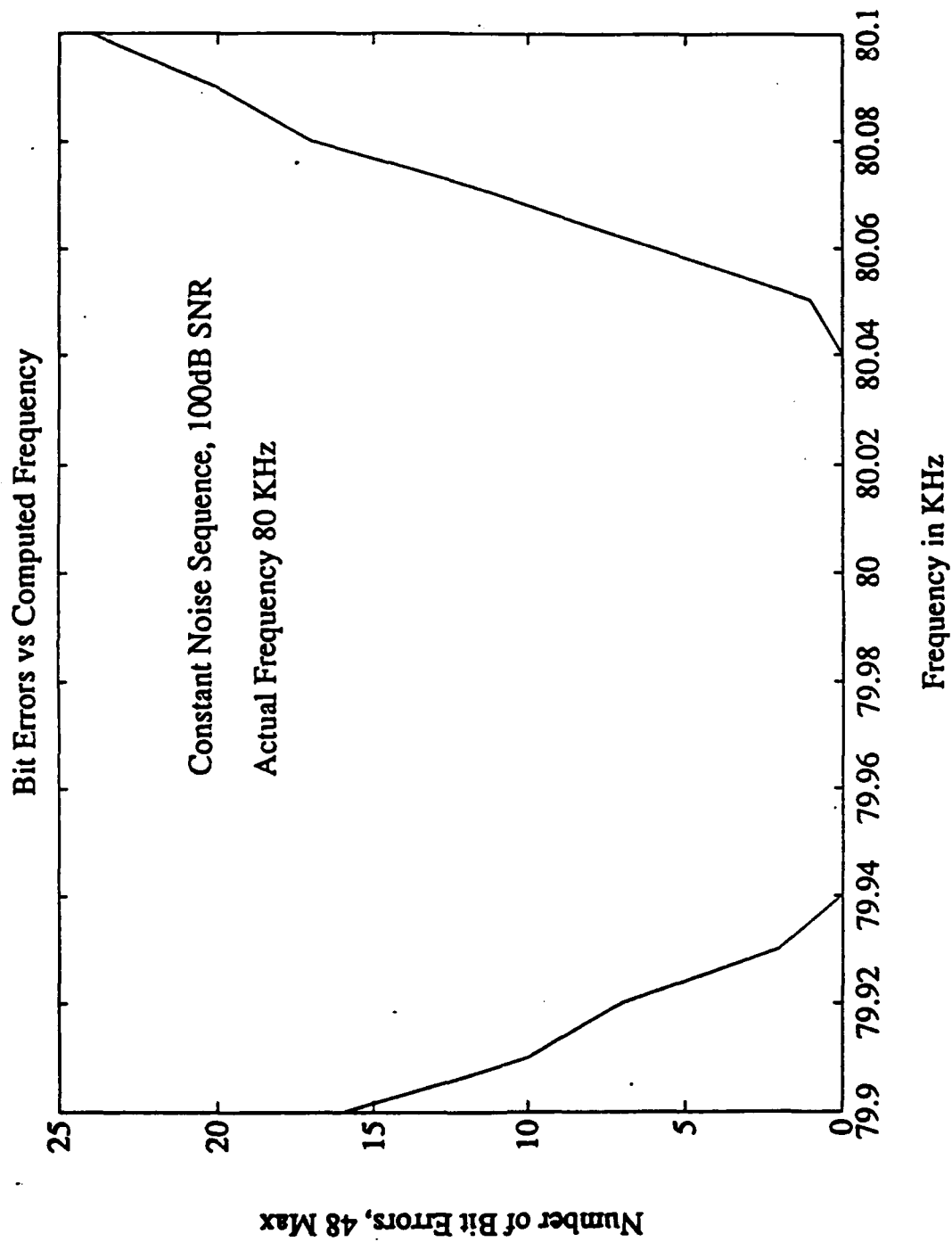


Figure 3-5. Accuracy Required to Demodulate BPSK Signals

## IV. SIMULATION RESULTS

### A. ACCURACY OF *ESPRIT*

The accuracy of the *ESPRIT* algorithm was investigated for a number of different cases. At the beginning of the investigation, the accuracy was first determined for the case of unfiltered white noise plus a cosine wave at 75 kHz and at a sampling rate of 300 kHz. *ESPRIT* was very accurate down to 0 dB with a variance of only 0.0445. The mean value was excellent even down to -15 dB. Figure 4-1 is a scatter graph of these results for 30 trials at each SNR.

Next, the accuracy was investigated for colored noise, i.e., noise that had been passed through the bandpass filter representing the hydrophone/preamplifier combination. Figure 4-2 is a scatter graph of the results using the same number of data points, carrier frequency, and sampling rate. As can be seen, the *ESPRIT* algorithm produces reasonably accurate results down to 0 dB. Below 0 dB, the variance increases significantly. Table 4-1 gives the estimated mean, variance, and standard deviation (SD) for both methods at each SNR.

TABLE 4-1. Comparison of *ESPRIT* Frequency Estimation

SNR(dB)	White Noise (Fig.4-1)			Colored Noise (Fig.4-2)		
	Mean	Variance	SD	Mean	Variance	SD
10	75.0027	0.0031	0.0557	75.0007	0.0025	0.0496
5	75.0058	0.0111	0.1054	75.0007	0.0080	0.0894
0	75.0121	0.0445	0.2110	74.9991	0.0276	0.1663
-5	75.0221	0.1966	0.4434	74.9937	0.1211	0.3480
-10	75.0279	0.7666	0.8756	74.9849	1.5850	1.2590
-15	75.0124	1.6515	1.2851	74.5513	19.0992	4.3703

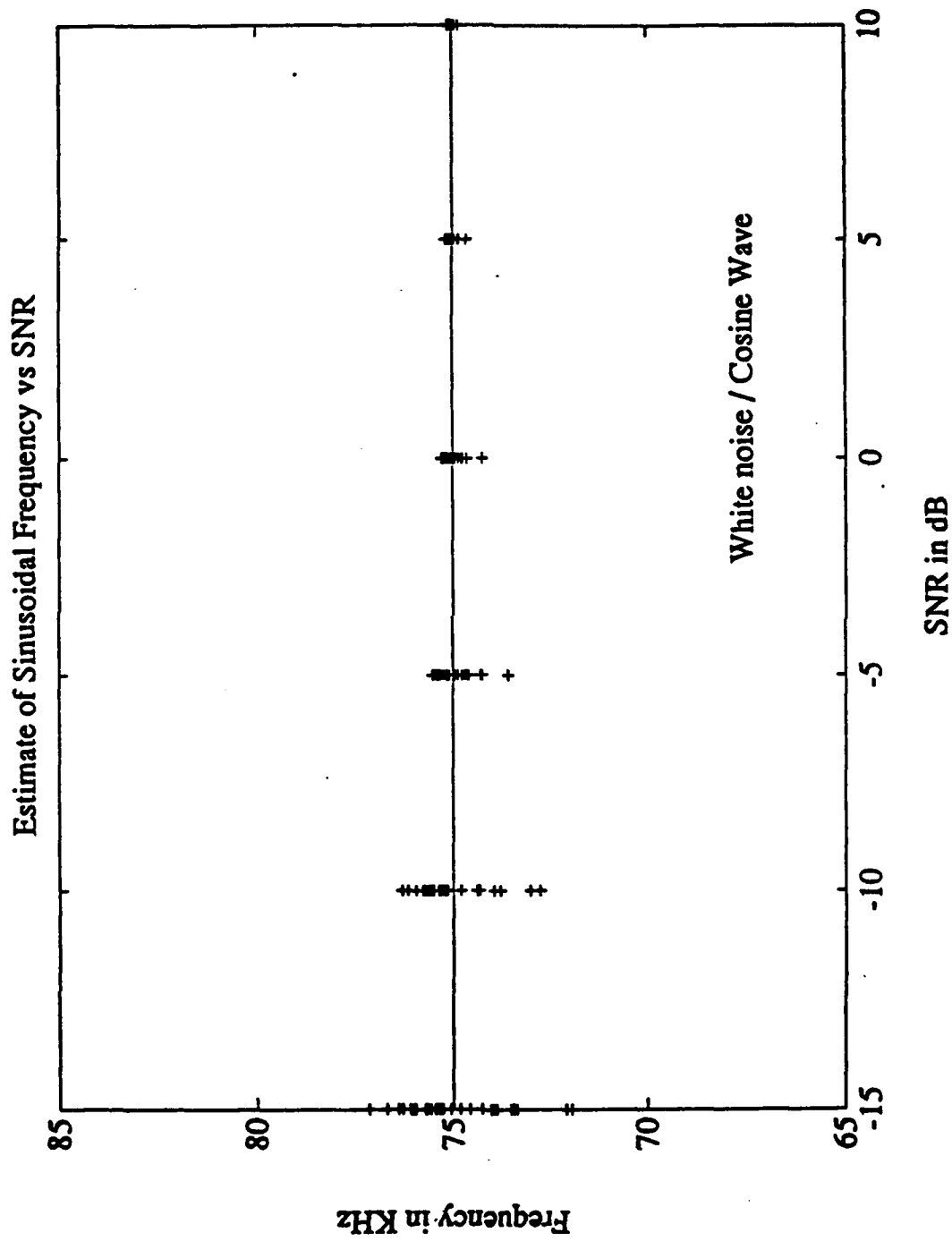


Figure 4-1. Accuracy of *ESPRIT*, White Noise

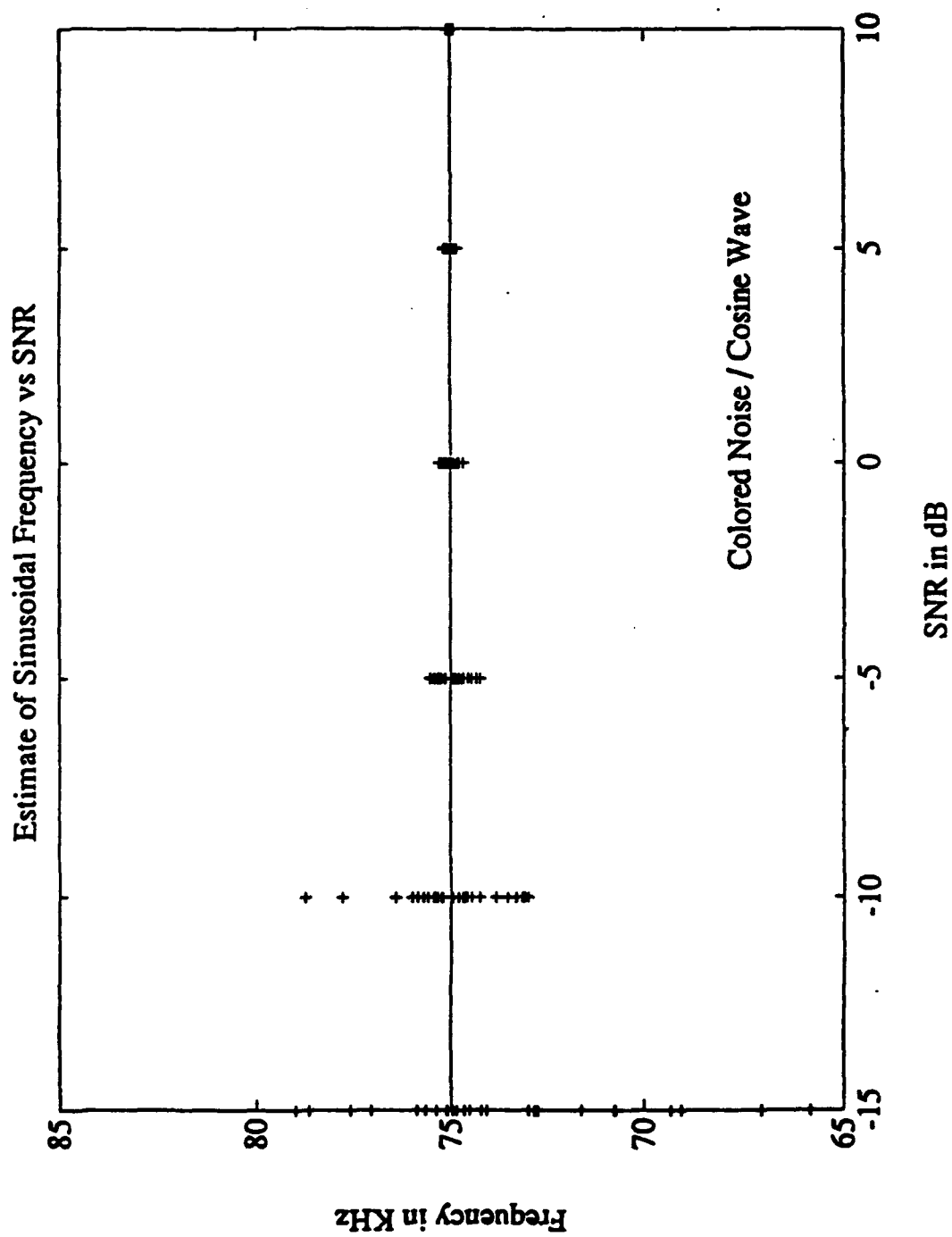


Figure 4-2. Accuracy of *ESPRIT*, Colored Noise

As a next step, we investigated the ability of *ESPRIT* to determine the received frequency of a BPSK modulated signal without doppler. For this case, the received frequency is equal to the carrier frequency of the transmitted signal. The sampling rate was set at 600 kHz, corresponding to eight times the carrier frequency. Each of the 47 individual bit intervals were processed separately to estimate the frequency. For each bit, 56 samples were used to do the estimation; the average of all the bits then gave the final result. If any of the frequency estimates did not fall within the range of 70 to 80 kHz, then that value was not included in the average. This produced the best frequency estimate possible. Figure 4-3 is another scatter graph showing the accuracy of the frequency estimate using this method. (Note that the vertical scale is not the same as that of Figures 4-1 and 4-2). As before, there were 30 trials for each SNR. During this portion of the investigation, it was observed that *ESPRIT* does not produce accurate estimates if the data used for the frequency estimate includes a phase shift between bits. When a phase shift is included anywhere within the data, the frequency estimated by *ESPRIT* was found to be in error by at least 1 kHz. This is unacceptable for any method of BPSK demodulation.

For the case of nonzero doppler, two methods were evaluated. The first of these methods used the first five bits of the BPSK signal to estimate the received frequency. This method was the first one attempted and depends on the fact that the first five bits are always a "1", therefore they do not contain any phase shifts. As stated previously, the accuracy needed for this method is very high. Specifically, the estimated frequency must be correct to within +40 Hz to -60 Hz. Figure 4-4 is a scatter graph showing the accuracy of this method for 30 trials at each SNR. It is clear that this method will not suffice even at a 10 dB SNR.

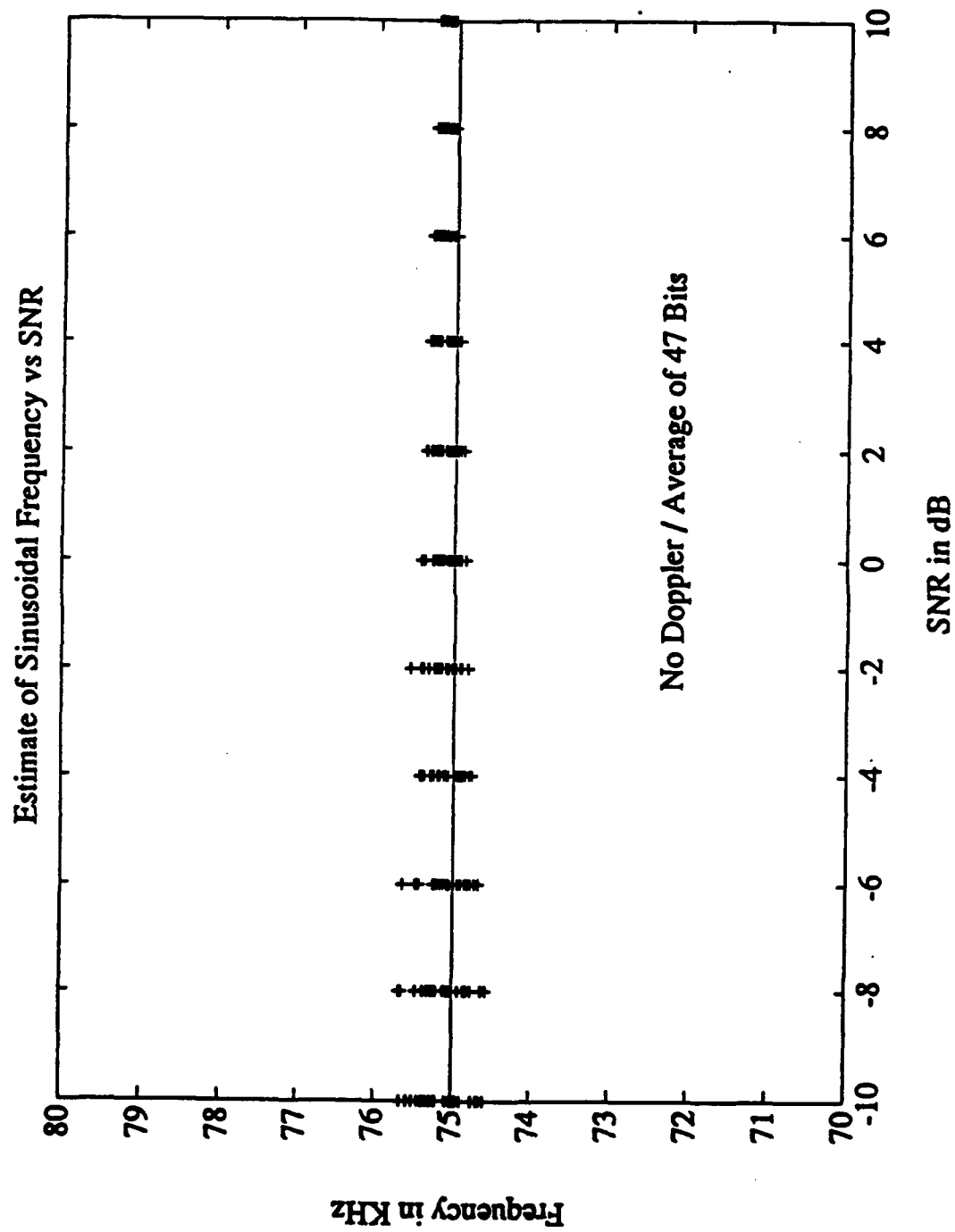


Figure 4-3. Accuracy of *ESPRIT*, No Doppler, Average of 47 Bits

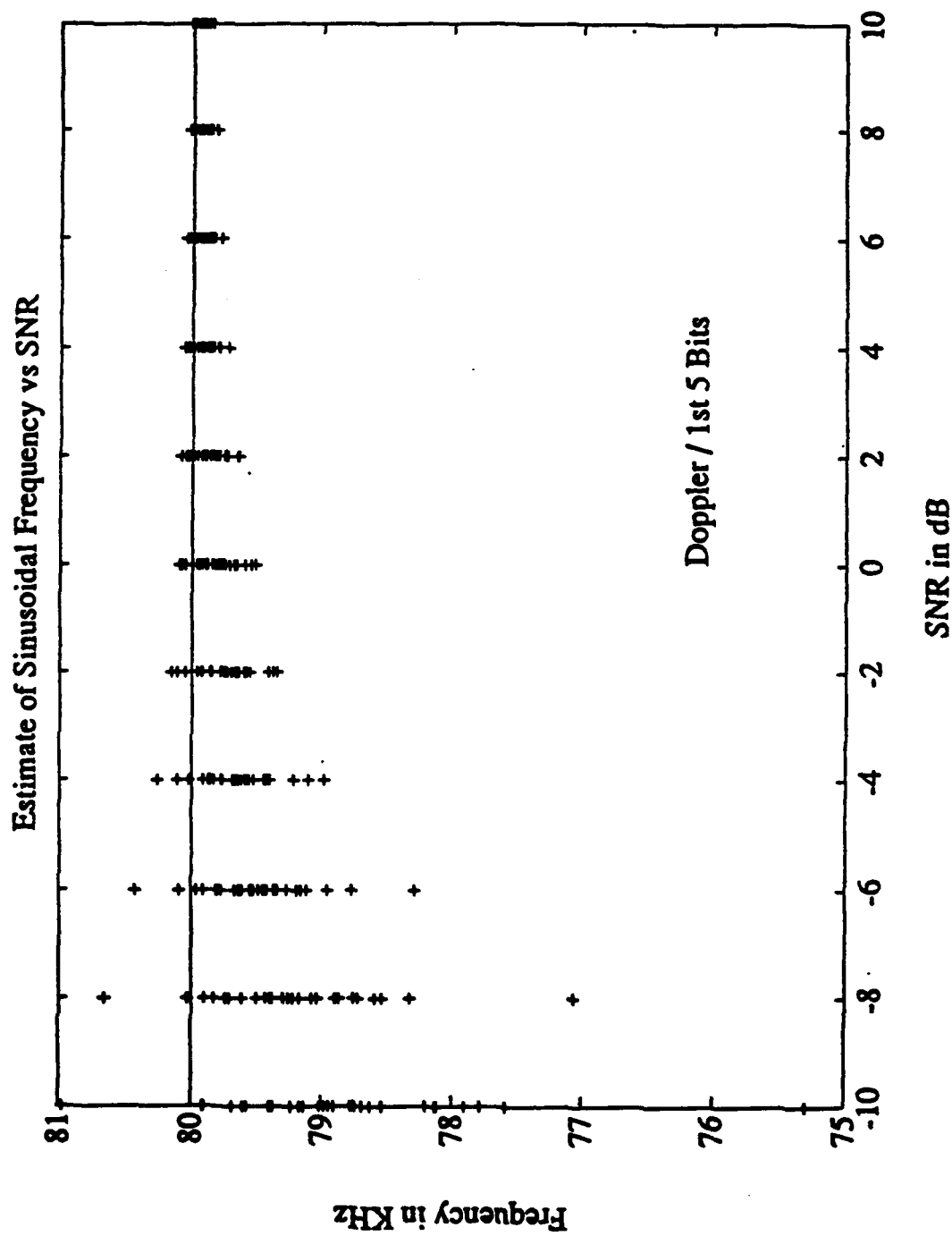
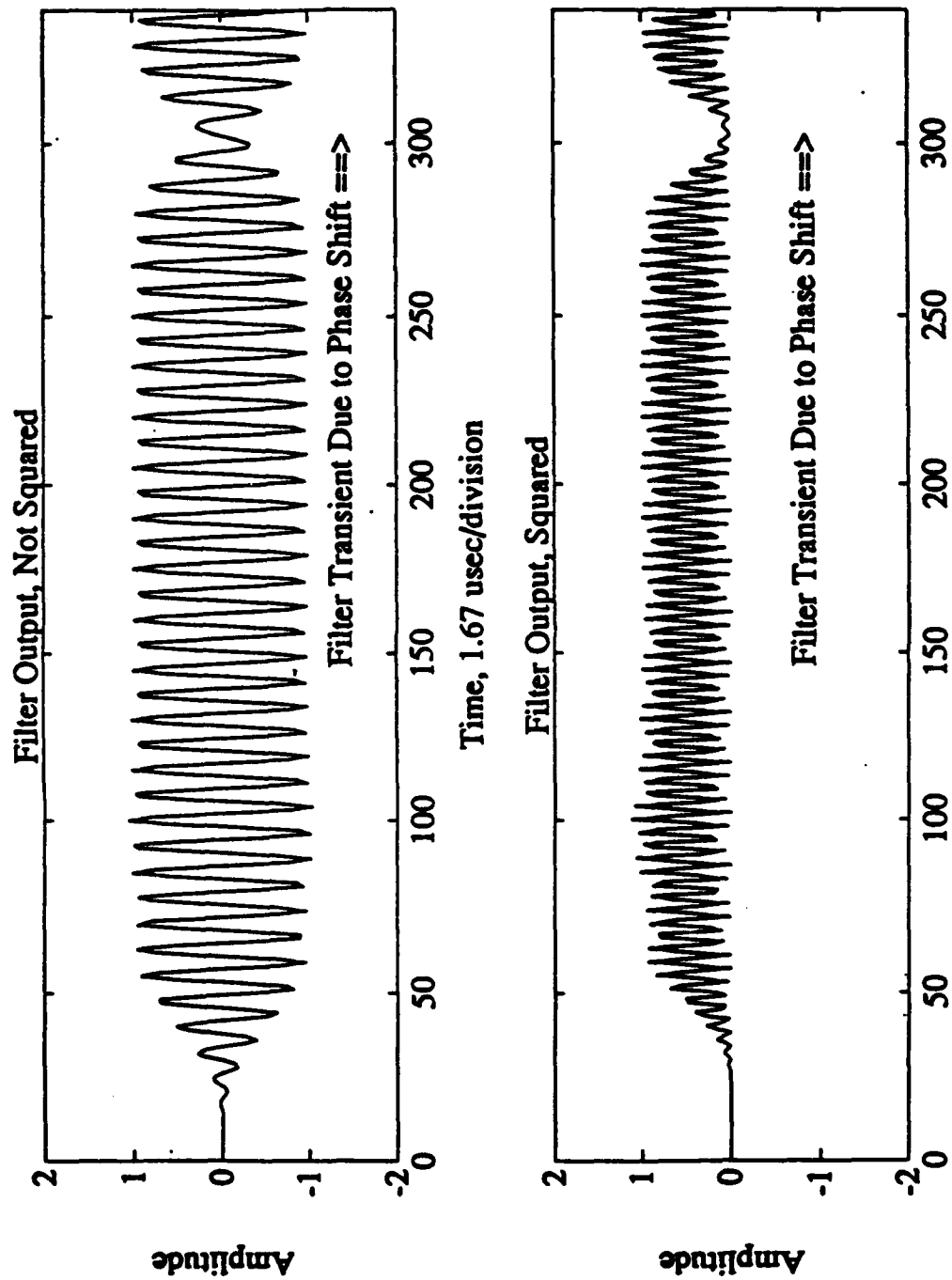


Figure 4-4. Accuracy of *ESPRIT*, Doppler, 1st 5 Bits

The next method investigated involves squaring the data after it passes through the bandpass filter. This method has the advantage in that it removes the phase shift between bits. However, even though the effects of the phase shift itself disappear, there is still a filter transient response that causes some distortion of the signal. Figure 4-5 is a plot of the filter output before and after the output is squared. For *ESPRIT*, the number of signals present increases because it is now necessary to detect the positive and negative frequency (at twice the received frequency) as well as the DC components. For this method, we applied the algorithm for  $M = 4$  to allow for possibly estimating the DC component as two frequencies very close to zero. To obtain the desired carrier frequency estimate, the double frequency estimate was halved, and the DC components were ignored.

A trade-off can be made between the number of samples used to form an estimate of the frequency and the number of such estimates that can be made and averaged in a given 47 bit transmission. Averaging more estimates (i.e. using shorter segments of data) tends to reduce the variance. A number of different combinations were attempted. The first of these methods used groups of three, five, or seven bit lengths of data and then averaged as many estimates as were available from the entire bit sequence. For example, if three bits worth of data are used for the frequency estimate, then there are  $\lfloor 47/3 \rfloor = 15$  frequency estimates that can be averaged together. For five bits worth of data, only  $\lfloor 47/5 \rfloor = 9$  frequency estimates can be averaged. As before, any estimates outside the expected range of 70 to 80 kHz were ignored in computing the average. Figures 4-6, 4-7, and 4-8 are the scatter graphs that show the accuracies of the three bit, five bit, and seven bit methods, respectively.



Time, 1.67 usec/division  
**Figure 4-5. Filter Transient Response Before and After Squaring**

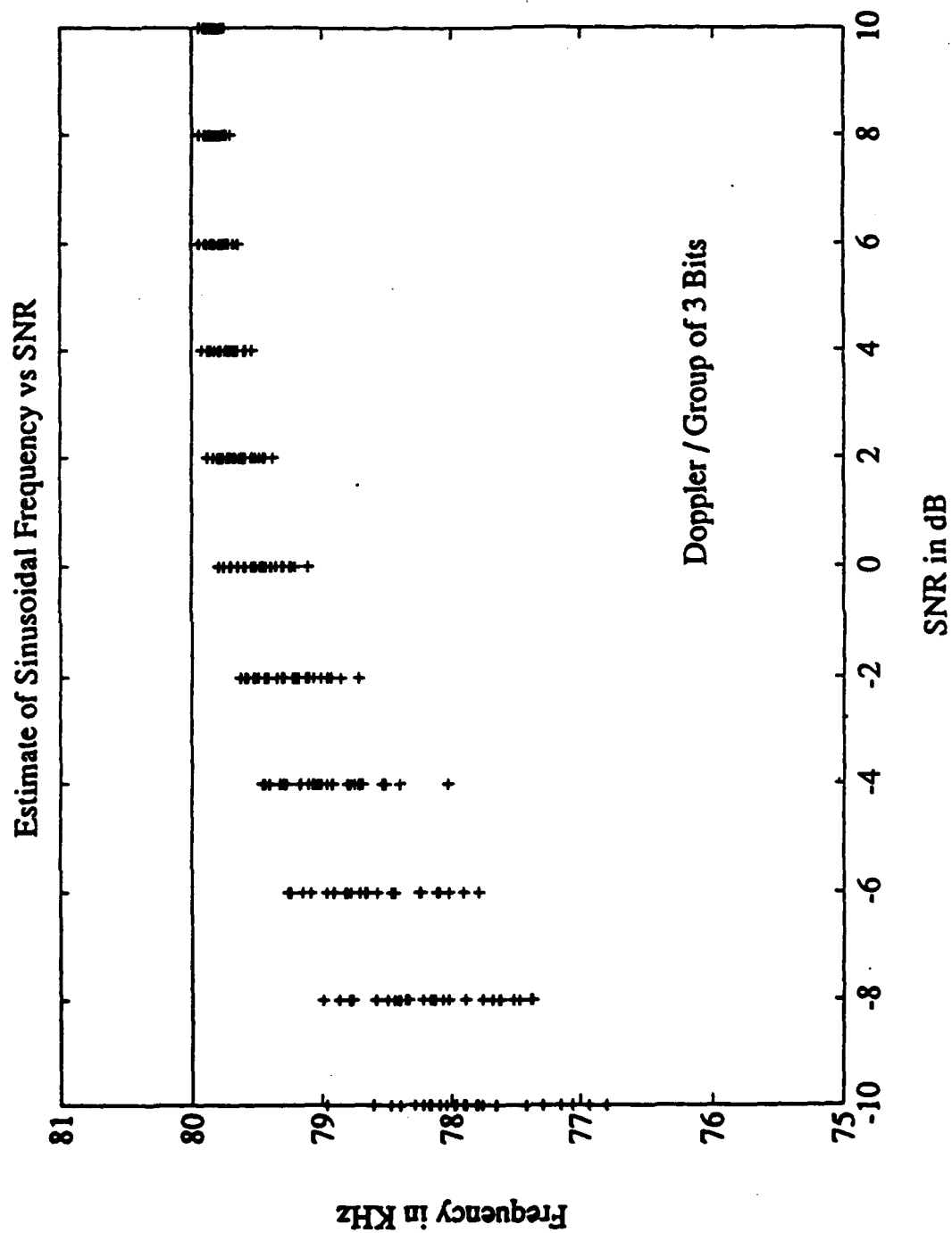
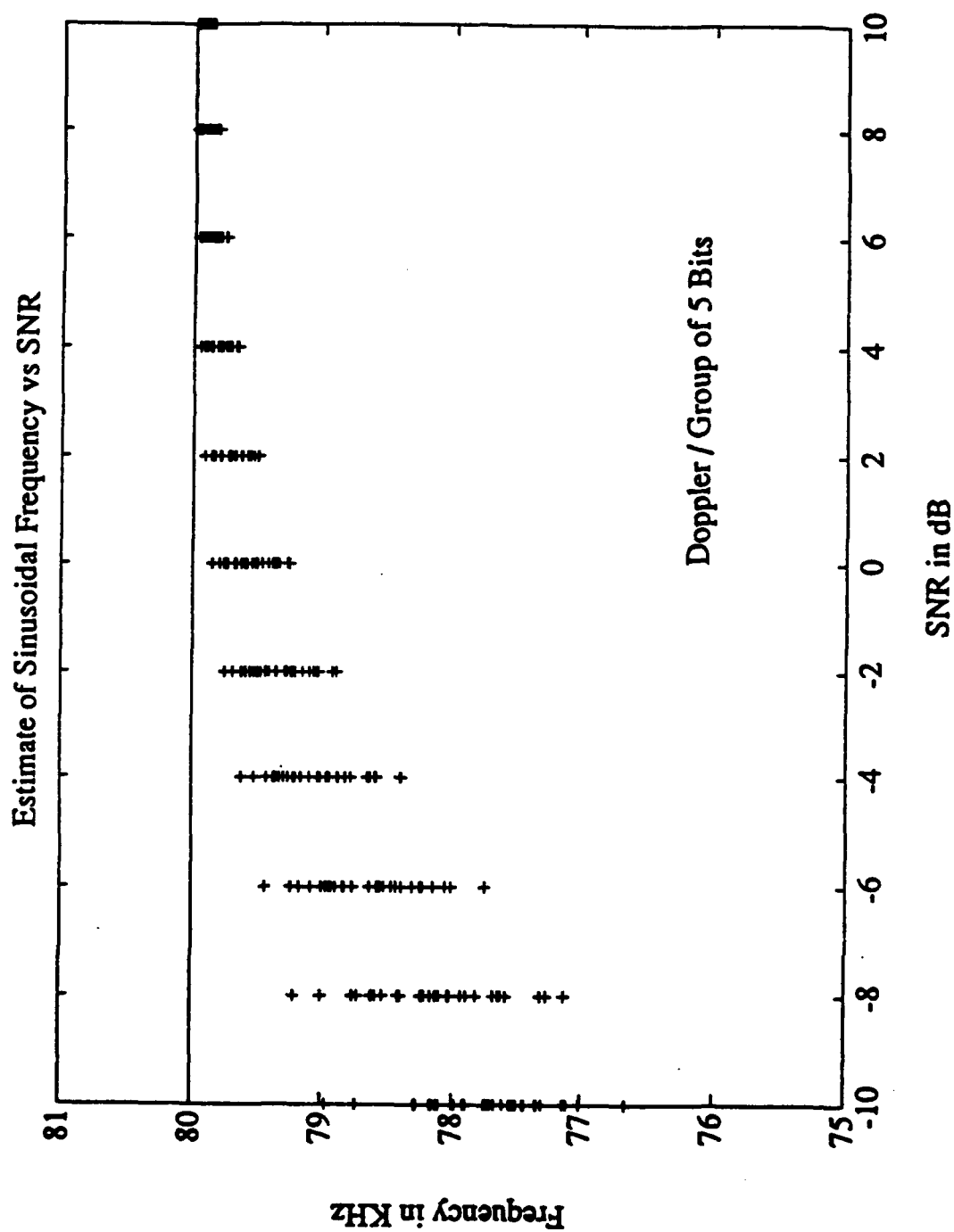


Figure 4-6. Accuracy of *ESPRIT*, Doppler, Groups of 3 Bits



**Figure 4-7. Accuracy of ESPRIT, Doppler, Groups of 5 Blits**

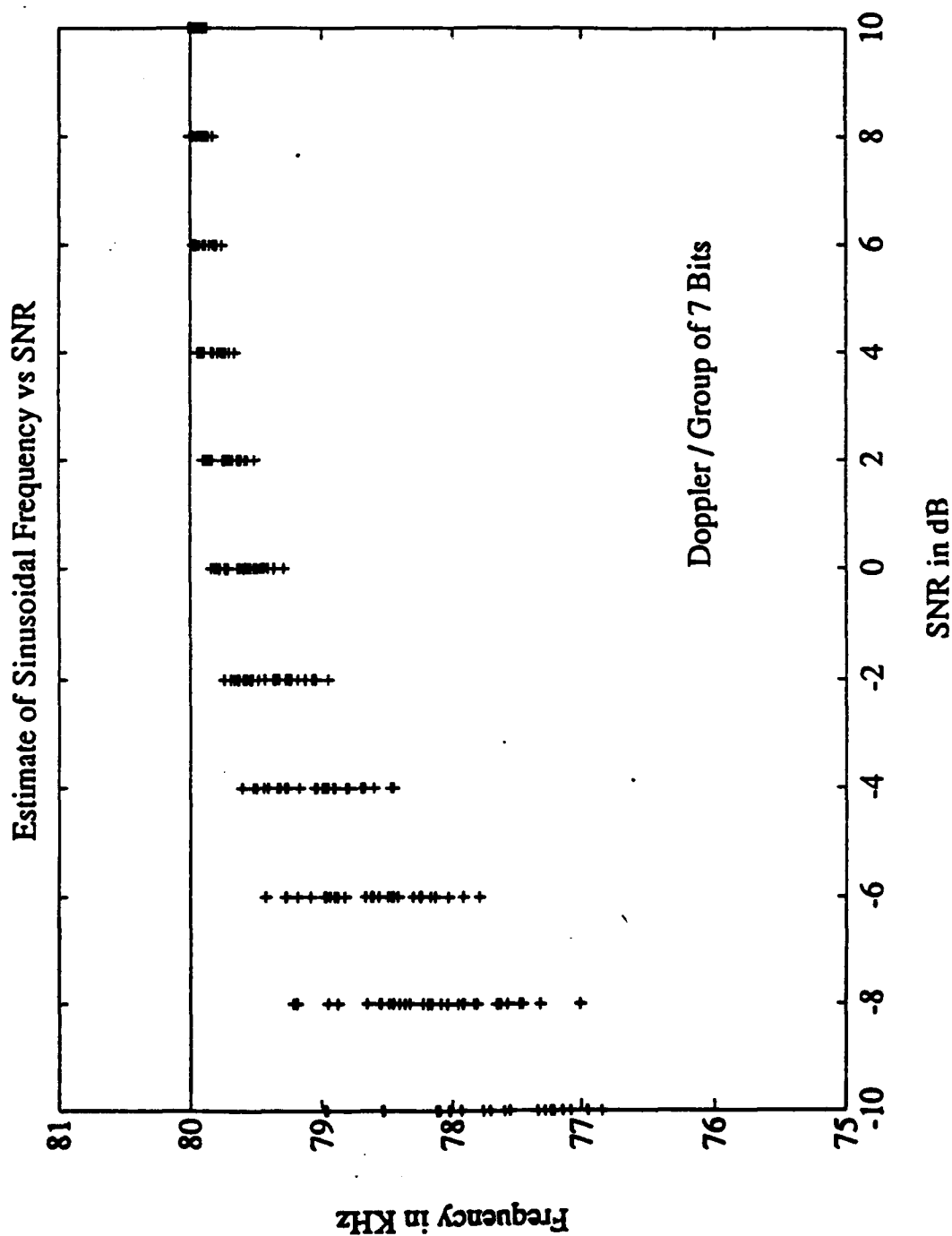


Figure 4-8. Accuracy of *ESPRIT*, Doppler, Groups of 7 Bits

The second method investigated involved the use of five bit lengths of data per segment by overlapping the segments to allow averaging a larger number of frequency estimates. For example, the first frequency estimate uses the squared data  $x(0)$  to  $x(261)$ , the second estimate uses the squared data  $x(157)$  to  $x(418)$ , and the third estimate uses  $x(313)$  to  $x(574)$ . This continues until the end of the bit sequence is reached. This allows the averaging of 15 estimates instead of the 9 used by the previous method. Figure 4-9 is a scatter graph of the results. The mean, variance, and standard deviation of the results in Figures 4-3, 4-4, and 4-6 to 4-9 are shown in Table 4-2 for comparison.

## **B. PROBABILITY OF BIT ERROR**

The previous section dealt exclusively with determining the accuracy of the frequency estimate. Since the ultimate objective is to use *ESPRIT* for BPSK demodulation in the presence of high noise levels, the bottom line is how well this method performs in the demodulation as compared to other known methods. The method by which we evaluated the overall performance is to calculate or experimentally estimate the  $P_e$ .

The method used to determine performance was to run a Monte Carlo type simulation for various SNR's. At each SNR, the total number of errors generated was divided by the total number of bits that were demodulated. This yields a  $P_e$  for each SNR. As long as the total number of bits demodulated is large, a reasonably accurate estimate of  $P_e$  should be attainable.

For the case of no doppler, the results show an outstanding capability in the presence of noise. Figure 4-10 is a graph of  $P_e$  vs SNR for this case. Compare this to Figure 4-11, a graph of the nominal  $P_e$  vs SNR for a standard analog BPSK receiver [Ref. 2:p. 246]. As is clearly shown, when doppler is not present, the decoding of BPSK signals using the

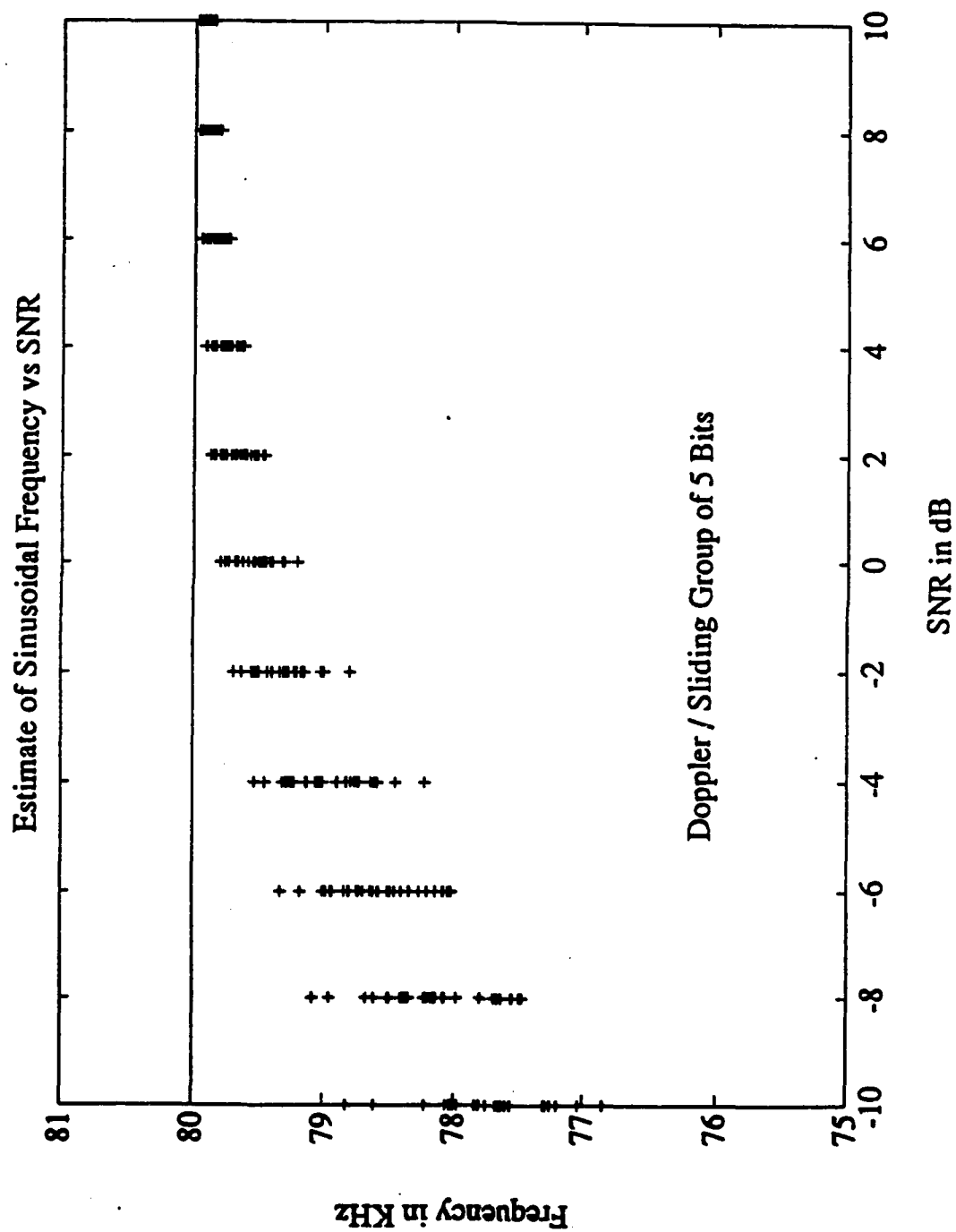


Figure 4-9. Accuracy of *ESPRIT*, Doppler, Sliding Group of 5 Bits

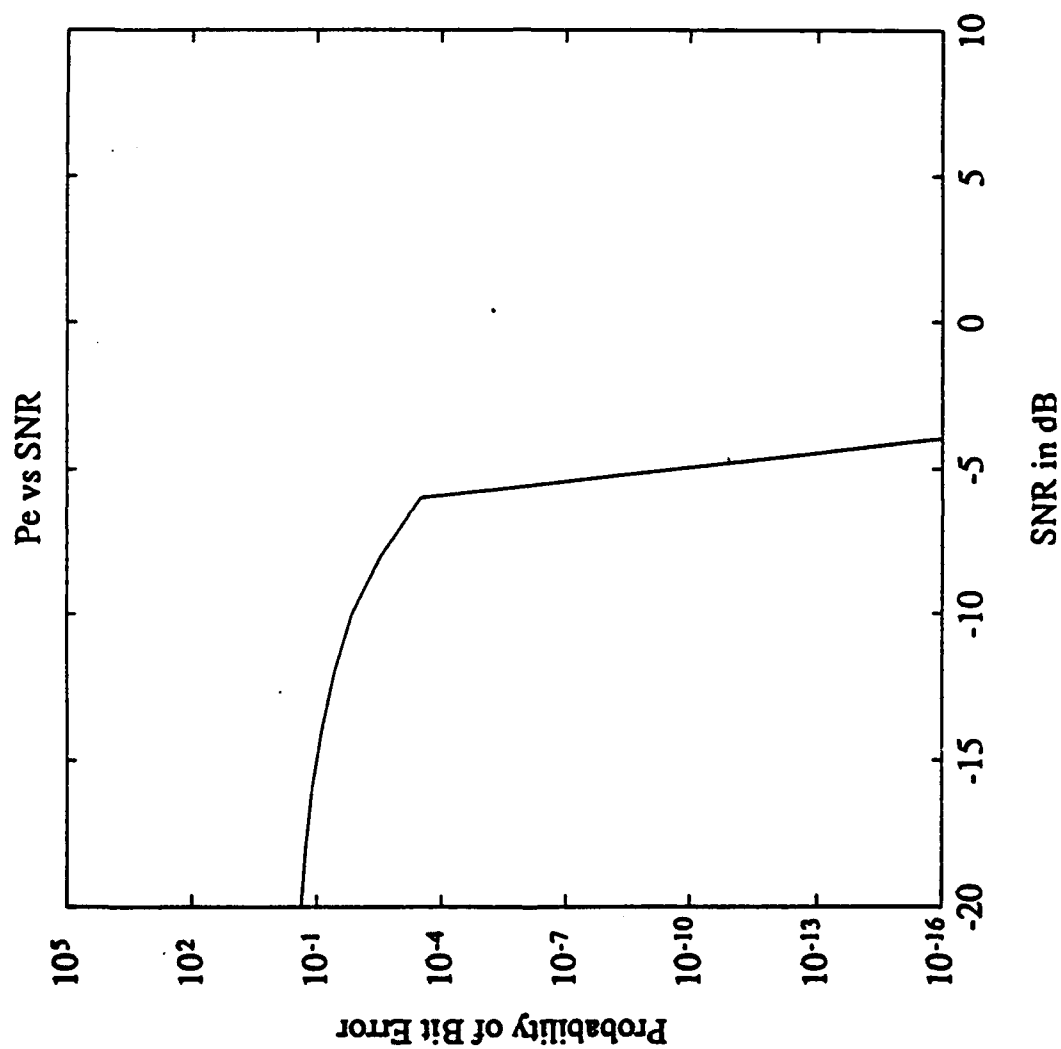


Figure 4-10. Probability of Bit Error for No Doppler

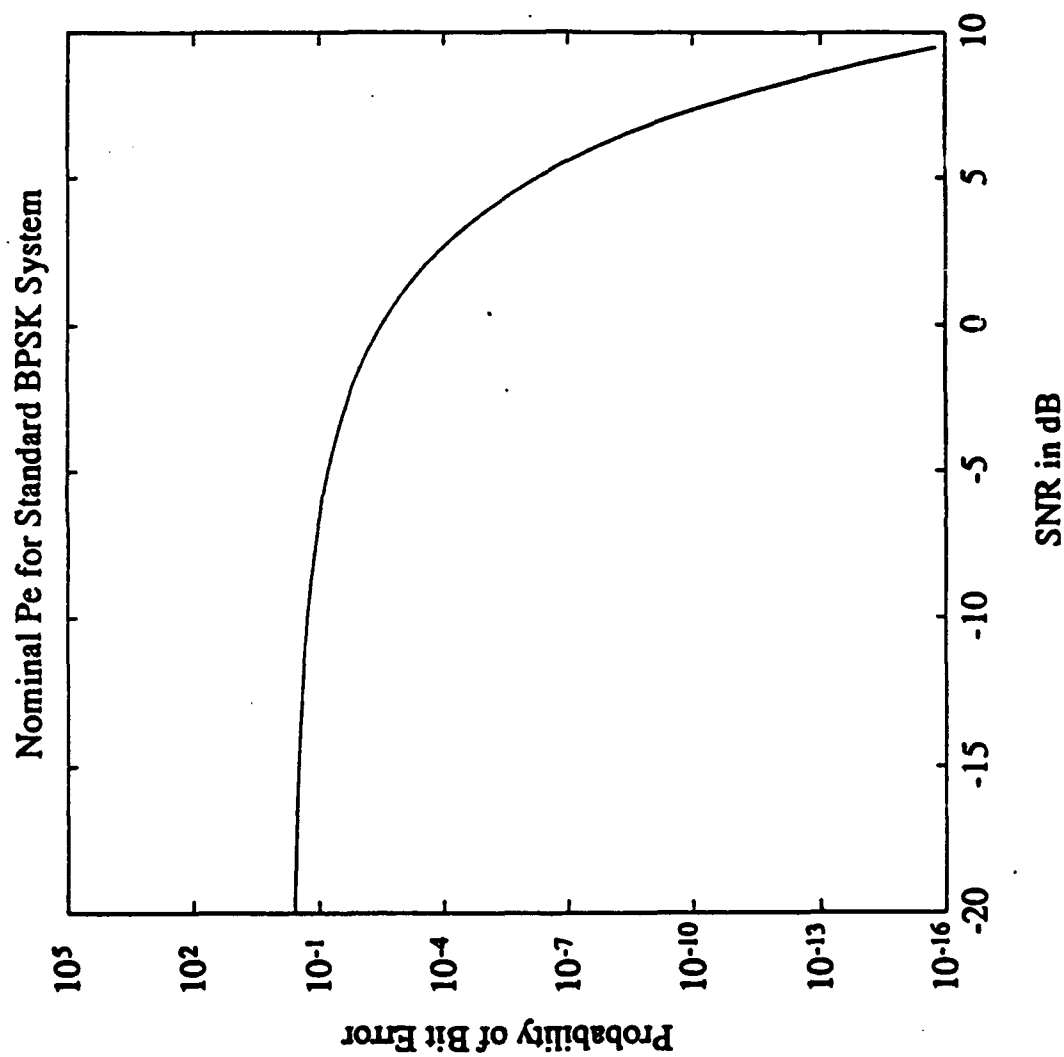


Figure 4-11. Probability of Bit Error for Nominal BPSK Receiver

*ESPRIT* estimate gives extremely low  $P_e$ . However, it is not clear that comparable results could not be obtained using a nominal value (i.e. 75 kHz) for the frequency instead of the *ESPRIT* estimate.

However, when doppler is present, there is a decrease in the performance of *ESPRIT* as compared to the standard receiver. Based on the results in Table 4-2, the method used to demodulate the BPSK signal was to use a sliding eight bit procedure similar to that discussed before for five bits. In this case, the group of eight bits were slid only one bit at a time so that a total of 40 frequency estimates were then averaged to arrive at the final estimate. This experiment resulted in very high error rates, as predicted by Figure 3-5, since the frequency estimates were not within the very tight tolerances shown in that figure. Notice that, from Table 4-2, the absolute accuracy of the frequency estimate (at 75 kHz) when there is no doppler is not any better than the estimates obtained when doppler is present. However, the fact that we do not need to compute the phase offset using the estimated frequency results in a better  $P_e$  for the lower degree of frequency estimate accuracy.

**TABLE 4-2. Comparison of ESPRIT Frequency Estimation**

SNR	No Doppler (Fig.4-3)			Doppler / 1st 5 Bits (Fig.4-4)		
	Mean	Variance	SD	Mean	Variance	SD
10	75.1356	0.0026	0.0511	79.9261	0.0015	0.0384
8	75.1304	0.0038	0.0614	79.9180	0.0024	0.0490
6	75.1350	0.0063	0.0794	79.9057	0.0040	0.0629
4	75.1294	0.0122	0.1107	79.8869	0.0066	0.0814
2	75.1242	0.0161	0.1267	79.8579	0.0114	0.1068
0	75.1011	0.0210	0.1451	79.8131	0.0303	0.1425
-2	75.1030	0.0348	0.1866	79.7435	0.0379	0.1948
-4	75.0662	0.0376	0.1939	79.6351	0.0758	0.2754
-6	75.0603	0.0628	0.2506	79.4659	0.1657	0.4071
-8	75.0770	0.0749	0.2737	79.2034	0.3962	0.6295
-10	75.1300	0.0892	0.2987	78.8114	0.9483	0.9738
SNR	Doppler / Group of 3 Bits (Fig.4-5)			Doppler / Group of 5 Bits (Fig.4-6)		
	Mean	Variance	SD	Mean	Variance	SD
10	79.8333	0.0019	0.0437	79.9213	0.0014	0.0375
8	79.8097	0.0031	0.0558	79.8959	0.0024	0.0487
6	79.7712	0.0056	0.0747	79.8557	0.0041	0.0640
4	79.7108	0.0097	0.0983	79.7928	0.0073	0.0856
2	79.6199	0.0161	0.1271	79.6955	0.0137	0.1168
0	79.4766	0.0300	0.1731	79.5467	0.0267	0.1634
-2	79.2603	0.0551	0.2348	79.3218	0.0533	0.2309
-4	78.9529	0.1212	0.3481	79.0032	0.1080	0.3286
-6	78.6237	0.1595	0.3994	78.5907	0.1756	0.4190
-8	78.1533	0.2083	0.4564	78.1461	0.2548	0.5048
-10	77.8452	0.2541	0.5041	77.7387	0.2490	0.4990
SNR	Doppler / Group of 7 Bits (Fig.4-7)			Doppler / Sliding 5 Bits (Fig.4-8)		
	Mean	Variance	SD	Mean	Variance	SD
10	79.9544	0.0013	0.0363	79.9079	0.0014	0.0375
8	79.9294	0.0022	0.0468	79.8822	0.0023	0.0483
6	79.8900	0.0037	0.0611	79.8417	0.0039	0.0627
4	79.8284	0.0066	0.0811	79.7771	0.0071	0.0844
2	79.7326	0.0121	0.1100	79.6778	0.0128	0.1133
0	79.5857	0.0233	0.1528	79.5284	0.0230	0.1516
-2	79.3656	0.0468	0.2163	79.2967	0.0465	0.2157
-4	79.0448	0.0990	0.3147	78.9747	0.0940	0.3065
-6	78.6277	0.1780	0.4219	78.5883	0.1239	0.3520
-8	78.1343	0.2923	0.5406	78.1151	0.1930	0.4393
-10	77.6609	0.3428	0.5855	77.7043	0.2115	0.4599

## V. CONCLUSIONS AND RECOMMENDATIONS

### A. CONCLUSIONS

As demonstrated by the experiments in Chapter IV, the *ESPRIT* algorithm can be depended on to give estimate accuracies on the order of  $\pm 0.5$  kHz down to 0 dB in the presence of noise and doppler. Accuracies to  $\pm 0.15$  kHz are obtainable with no doppler present. However, in order to accurately demodulate BPSK signals when doppler is present, the frequency must be within +0.04 kHz to -0.06 kHz. We were not able to achieve such high accuracies in this application of *ESPRIT*.

### B. RECOMMENDATIONS

Although our experiments were not able to produce a sufficiently high-accuracy frequency estimate to permit effective decoding of the signal in a high noise environment, the algorithm may have some use if appropriate filtering is employed to reduce the noise. Experiments with an adaptive filter [Ref. 5] showed reasonable success in reducing noise to effectively demodulate the signal. A combination of this adaptive filtering with a frequency estimation algorithm based on *ESPRIT* may therefore be worthy of further investigation.

## LIST OF REFERENCES

1. Roy, Richard H., *Estimation of Signal Parameters via Rotational Invariance Techniques*, Ph.D.Dissertation, Stanford University, Stanford, California, 1989.
2. Proakis, John G., *Digital Communications*, 2d ed., McGraw-Hill Book Company, 1989.
3. Therrien, Charles W., *Discrete Random Signals and Statistical Signal Processing*, Prentis-Hall Inc, 1992.
4. Golub, G. H. and Van Loan, C. F., *Matrix Computations*, Johns Hopkins University Press, 1984.
5. Herdegen, Dale, *Adaptive Noise Cancellation Applied to the NUWES Test Range*, Master's Thesis, Naval Postgraduate School, Monterey, California, December 1991.

## INITIAL DISTRIBUTION LIST

	No. Copies
1. Defense Technical Information Center Cameron Station Alexandria, Virginia 22304-6145	2
2. Library, Code 52 Naval Postgraduate School Monterey, California 93943-5002	2
3. Chairman, Code EC Department of Electrical and Computer Engineering Naval Postgraduate School Monterey, California 93943-5000	1
4. Professor Charles W. Therrien, Code EC/Ti Department of Electrical and Computer Engineering Naval Postgraduate School Monterey, California 93943-5000	3
5. Professor Murali Tummala, Code EC/Tu Department of Electrical and Computer Engineering Naval Postgraduate School Monterey, California 93943-5000	1
6. Mr. John Hager (Code 70E1) Naval Undersea Warfare Center Keyport, Washington 98345	2
7. Lt Charles H. Wellington Jr. 1047-A Highland Street Seaside, California 93955	1
8. Capt. Dale Herdegen 9757 Ideal Avenue North Mahtomedi, Minnesota 55115	1
9. Lcdr. John B. Scout 476 Century Vista Dr. Arnold, Maryland 21012	2